CONTENTS

1. STATISTICAL ANALYSIS OF THE ERRORS IN THE EXPERIMENTS 2

1.1 INTRODUCTION 2
1.2 METHOD 2
1.2.1 Analysis of uncertainties 2
1.2.2 Data sample 4
1.2.3 Oscillations 4
1.3 RESULTS 5
1.3.1 Mixed ventilation flows 5
1.3.2 Heat gains from solar radiation - EXP-14-11-00 13
1.3.3 Plain and deflector set-up for hot air supply- EXP-30-11-00 & EXP-1-12-00 16
1.3.4 High input rates - EXP-5-12-00 19
1.3.5 Low and high input rates - EXP-8-12-00 21
1.3.6 Low input rates - EXP-11-12-00 23
1.4 DISCUSSION 24
1.4.1 Signal description 25
1.5 SUMMARY 26

1. Statistical Analysis Of The Errors In The Experiments

1.1 INTRODUCTION

The statistical properties of the experiments are calculated and analysed. The flows in buildings are generally considered as steady state. However, there is no general proof to describe the extent of the average magnitude of the instabilities that occur at stabilising conditions. The deviation associated with special flows in buildings is obtained for several cases for generally high level of confidence. The manual collection of the values has proved to be generally good which is higher than 90% in several cases. Any frequency modes that occur are low when the flow is stabilised and do not affect match the accuracy.

In most situations, the convergence is governed by the reduction to the fluctuations of the mean value. However, this may be affected by small external disturbances even in controlled environments depending on the size of disturbance and insulation. This can lead to independent cases of convergence within relatively small limits of variance for certain time periods. This yields the deviations for the change of the mean value that is obtained every 2min σ_e and σ_m that is obtained from the mean every 15 min which varies slightly with different case. By looking at each experimental case individually, both σ_m and σ_e can give a good approximation of the magnitude of the instabilities that occurs in buildings. Taking a close snapshot to a stratified flow field, the buoyancy forces are small compared to the viscous forces. In all temperature-related problems for weak stratification, the following relation is true,

$$\frac{\partial T}{\partial t} \propto \rho u_j \nabla u_i \tag{1.1}$$

In this basis, the small-scale temperature distribution follows the turbulent velocity field. To monitor these changes is possible by looking at the table of the σ_{rms} values with height as obtained from the horizontally located thermocouples. The mean is obtained by integration with height. The values are then mapped to a table of confidence levels by a program. Looking at the average of the values across the height may not be enough depending on the case. The horizontal values are also plotted because they also describe the convergence of the results.

1.2 METHOD

1.2.1 Analysis of uncertainties

The variance for the total amount of data is govern by the equation,

$$ss_{tot} = ss_{Set1} + ss_{Set2} + \ldots + ss_{error1} + ss_{error2} + \ldots + ss_{mn} \tag{1.2}$$

where ss_{Set1} and ss_{Set2} are the variances obtained from similar Th.Sets. The variances of the errors form the two Sets are ss_{error1} and ss_{error2}.

The total deviation of the mean value or the error is obtained by calculating the individual deviations across the horizontal layer after the temperature readers are stabilised. The deviation obtained from the readings at the particular horizontal array of thermocouples at j is calculated from the square root of the sum of the square of the errors as below,

$$s_j = \sqrt{\frac{1}{(n-1)}\left[\sum_{i=1}^{n} y_i^2 - \frac{1}{n}\left(\sum_{i=1}^{n} y_i\right)^2\right]}. \tag{1.3}$$

There are several constraints affecting the accuracy of the measurements. The distribution changes with height, the umber of degrees of freedom and the convergence have to be accessed too. Due to the difference in the deviation of the temperature values with height, the rms-mean deviation is obtained by integrating with room height,

$$\sigma_{rms} = \sqrt{\frac{1}{|a-b|}\sum_{a}^{b} s_j^2 \delta x} \tag{1.4}$$

where a is the height of the first thermocouple and b is the height of the highest thermocouple. The average deviation across the height is evaluated by using the trapezoidal rule, which for the case of equal heights, can be written as follows,

$$I = \sum_{a}^{b} s_j^2 \delta x = h\left(\frac{1}{2}s_1^2 + s_2^2 + \ldots + s_{n-1}^2 + \frac{1}{2}s_{12}^2\right) \tag{1.5}$$

to calculate the confidence intervals across the height and establish an idea about the coverage of the values, the deviation s_j needs to be compared to the mean deviation.

In many engineering applications, a confidence level of larger than 60% would be considered acceptable. The deviation of the mean is also assisted by graphical plot of the mean deviation, s_i, for each sample of 12 temperature values, versus time and measurement. The ±0.1°C accuracy range previously evaluated by the calibration tests which is equal to 2σ can be higher or lower in the experimental cases depending on the number of values. To access the convergence of the error is done by calculating the confidence range at each level of thermocouples. This is done from the values obtained by each thermocouple and it is calculated by using the formula below,

$$z_{ei} = \frac{2 \times \sigma_e}{s_{ei}} \tag{1.6}$$

after having acquired the values for the error range, z_e, the confidence level, $c.l._e$, is obtained by mapping this parameter onto a probability table, such as student's table, which can also take into account the effect of the number of values. The errors can follow any distribution with height as a function of the flow conditions. Hence, the values are integrated with height to yield the rms-mean confidence level.

No experiment can run in perfectly stable conditions. Heat losses by conduction and mass leakage can occur through walls and adventitious openings due to stack effects. In

a temperature-controlled environment, this is limited within acceptable values. For the environmental chamber in this work, these heat losses are less pronounced, but they still affect the accuracy and the stability of the experiment.

The experimental stability level, $c.l._m$, is also expressed in terms confidence level, similar to the $c.l._e$, and it shows how much the mean values change between samples. The samples are collected from 12 values across the height from each thermocouple. The equation of the experimental stability is defined form the equation below,

$$z_{m_i} = \frac{2 \times \sigma_m}{s_{m_i}} \tag{1.7}$$

where z_m is calculated using the student's table in order to include the effect of the degrees of freedom in the confidence level. The parameter $c.l._m$ is obtained by mapping z_m onto student's table. Small significance levels signify that the results have been little affected by external sources.

1.2.2 Data sample

Additional to the equation given above for the analysis of convergence, the convergence is also affected by the sample size. The data considered may not be enough to eliminate any dependencies on the number of degrees of freedom. The sample size and precision of the equipment are very important in the manual collection of measurements. The accuracy is governed by the equation of uncertainty range as given below,

$$\Delta = \frac{2 \times \sigma_p}{\sqrt{n}} \tag{1.8}$$

where σ_p is the precision of the instrument, Δ is the required accuracy range that can be achieved if n number of readings are obtained for each sample. In the analysis of the deviation in this work using this formula a minimum of 25 readings need to be collected in order to achieve a range of accuracy equal to 0.04. Almost twice as many values are used for each deviation value across the horizontal calculation for a single Th.Set. Taking a single reading could introduce further errors in the analysis. To enhance the accuracy is done by taking the mean value through a series of readings.

1.2.3 Oscillations

Although convergence may occur, the temperature distribution changes slightly with time. These occur in several modes of which the most important ones have been recorded when taking the measurements. The behaviour of the temperature distribution with time can be depicted in Figure 1.1 below,

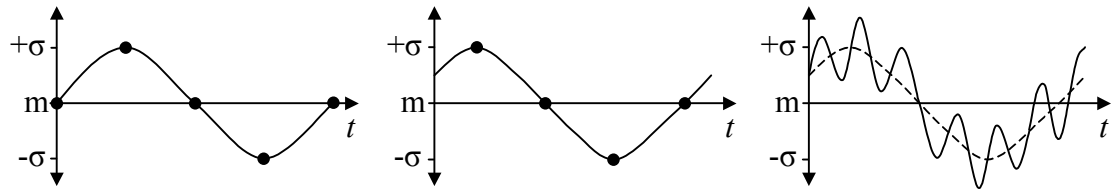

Figure 1.1: Fluctuation of the mean. In (a), ideal case of the fluctuation of mean value. In (b), typical fluctuation of mean value for no error case. In (c), an approximate representation of real case.

The results in Figure 1.1 (b) can be looked at as the deviation of a mean value. The likelihood for the sample mean to occur is 2 by making a typical measurement of a mean. The average is denoted by the number N_1 in the tables of this work. Each dot could signify a small sample reading that is usually obtained from several measurements with time. The average value is denoted as N_2 in the tables of this work. The deviation of the mean is denoted as σ_m which is the total deviation that is obtained from each data set that is collected at the different instances from each Th.Set. The deviation of the error is denoted as σ_e which is the total deviation that is calculated form the sample-readings at each instance.

Each measurement is an average over the period of 5-10sec over a range of several measurements.

1.3 RESULTS

1.3.1 Mixed ventilation flows

These experimental cases were carried out to test what is the effect of mixing in the environmental chamber. There were four cases. The first two cases were carried out with a hot air supply from the top and an ambient air supply at the bottom of the environmental chamber. That was done to test the response of the chamber medium at different temperatures. There were another two tests carried out with only the ambient air supply, in order to test the chamber response at smaller flow rates and temperatures. Slightly varying the extract height did not make any obvious difference, probably due to the high mixing involved with these cases.

The data is split and analysed into three regions as well as the entire range is analysed as it follows below,

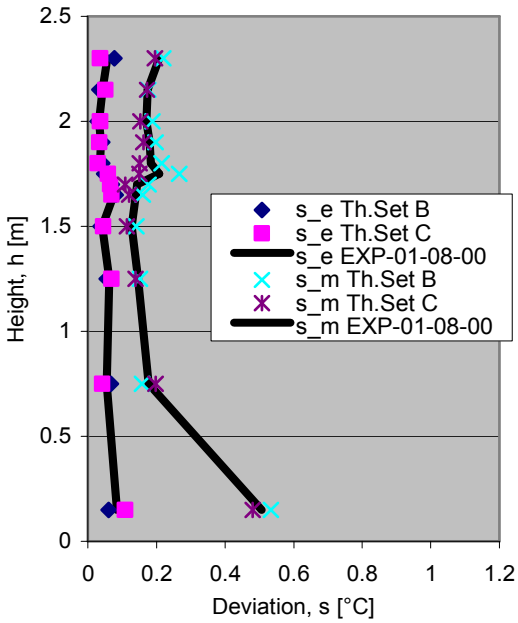
Height, h [m]
Deviation, s [°C]
s_e Th.Set B
s_e Th.Set C
s_e EXP-01-08-00
s_m Th.Set B
s_m Th.Set C
s_m EXP-01-08-00

(a)

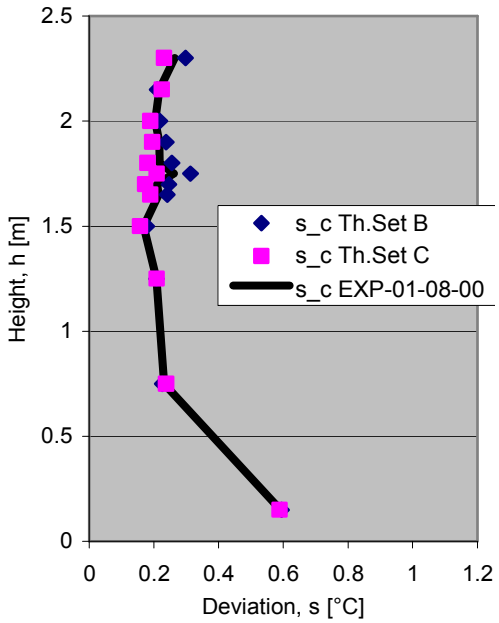
Height, h [m]
Deviation, s [°C]
s_c Th.Set B
s_c Th.Set C
s_c EXP-01-08-00

(b)

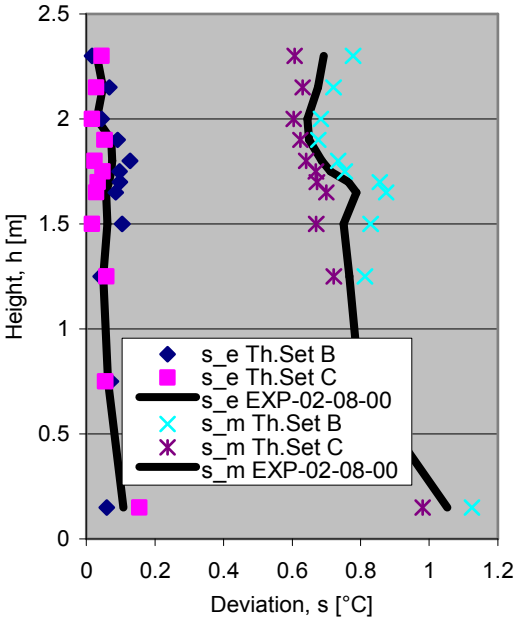
Height, h [m]
Deviation, s [°C]
s_e Th.Set B
s_e Th.Set C
s_e EXP-02-08-00
s_m Th.Set B
s_m Th.Set C
s_m EXP-02-08-00

(c)

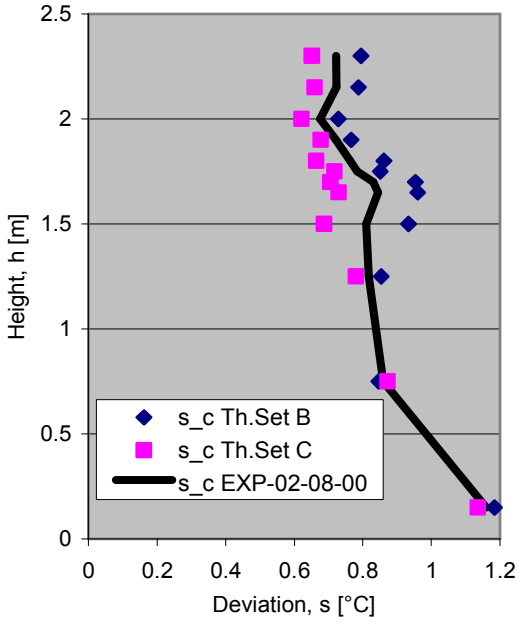
Height, h [m]
Deviation, s [°C]
s_c Th.Set B
s_c Th.Set C
s_c EXP-02-08-00

(d)

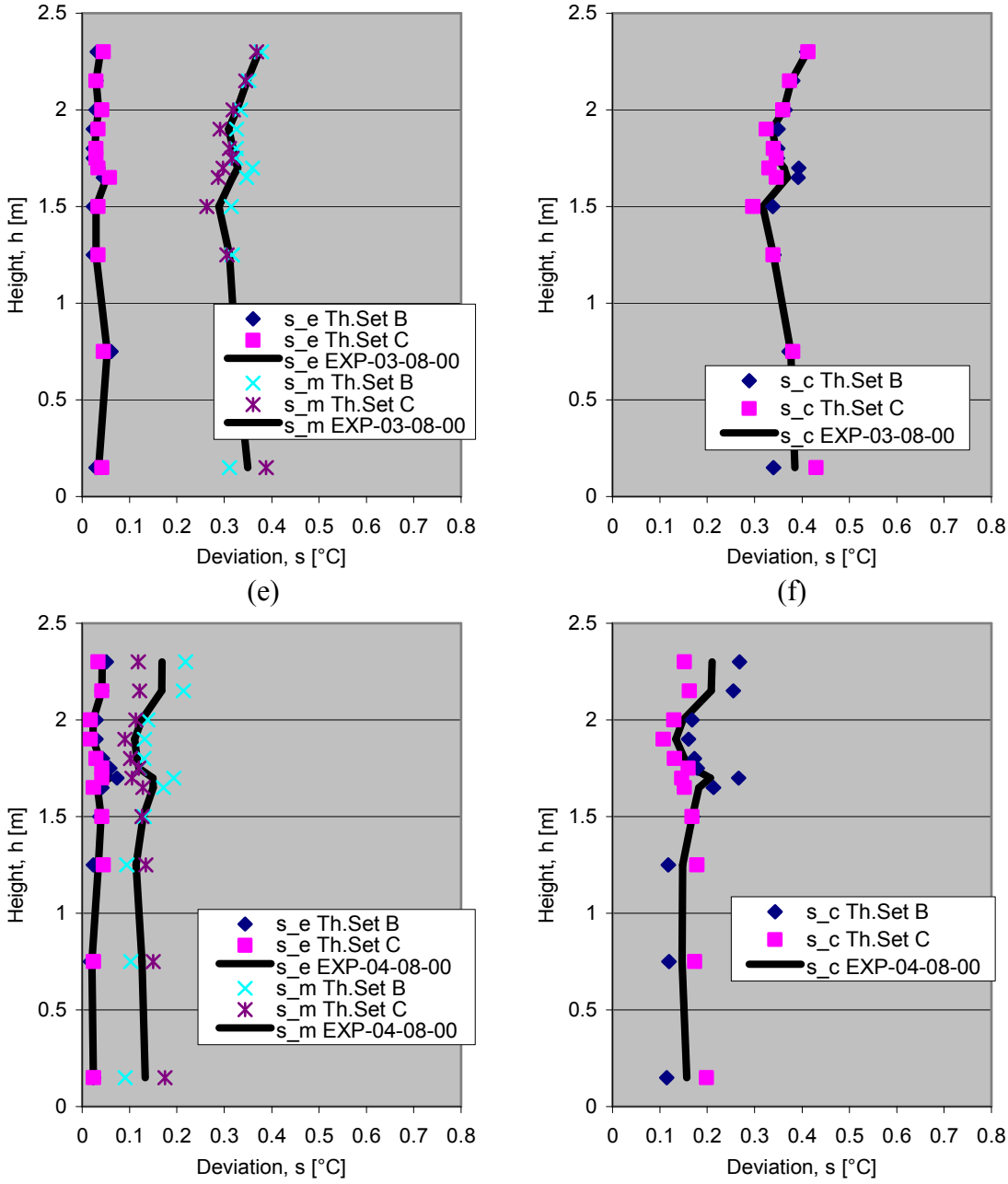

Figure 1.2: Error deviations for high and low frequencies form the experimental cases of (a)&(b) EXP01, (c)&(d) EXP02, (e)&(f) EXP03 and (g)&(h) EXP04.

The temperature variation away form the supply jets is analysed in the last two rows of the chamber grid as it follows below,

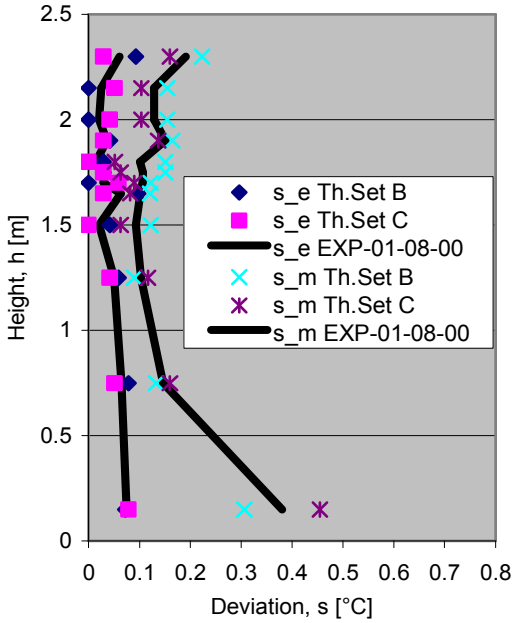
Height, h [m]
Deviation, s [°C]
s_e Th.Set B
s_e Th.Set C
s_e EXP-01-08-00
s_m Th.Set B
s_m Th.Set C
s_m EXP-01-08-00

(a)

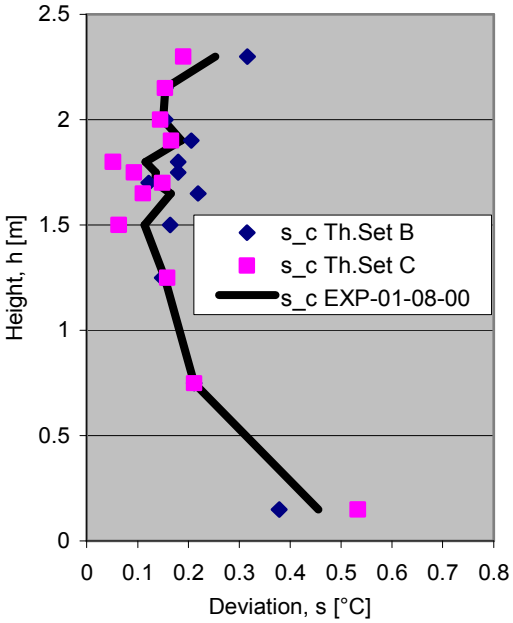
Height, h [m]
Deviation, s [°C]
s_c Th.Set B
s_c Th.Set C
s_c EXP-01-08-00

(b)

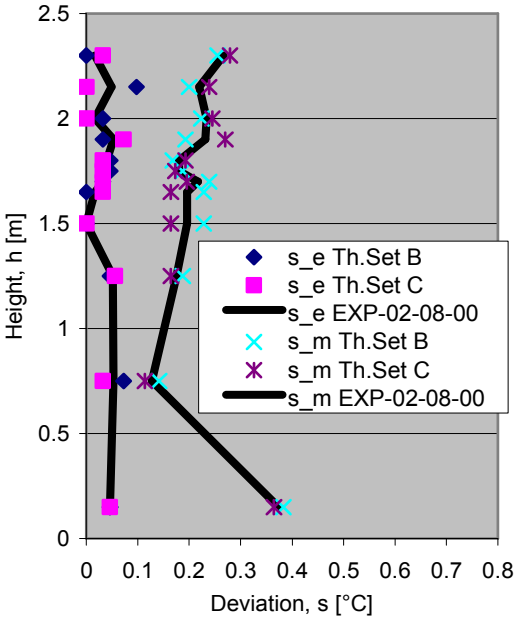
Height, h [m]
Deviation, s [°C]
s_e Th.Set B
s_e Th.Set C
s_e EXP-02-08-00
s_m Th.Set B
s_m Th.Set C
s_m EXP-02-08-00

(c)

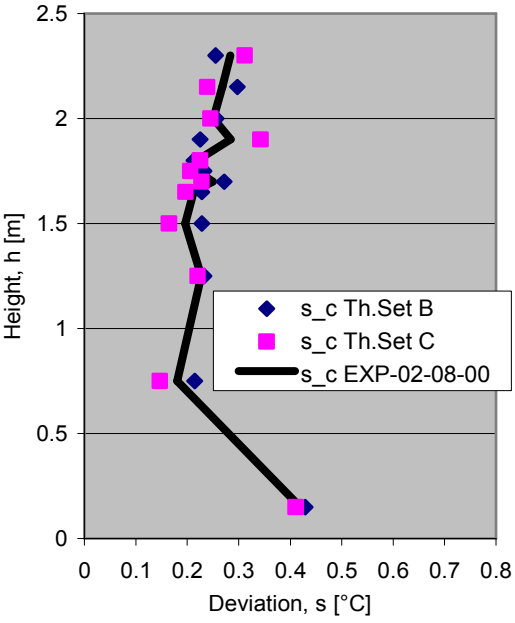
Height, h [m]
Deviation, s [°C]
s_c Th.Set B
s_c Th.Set C
s_c EXP-02-08-00

(c)

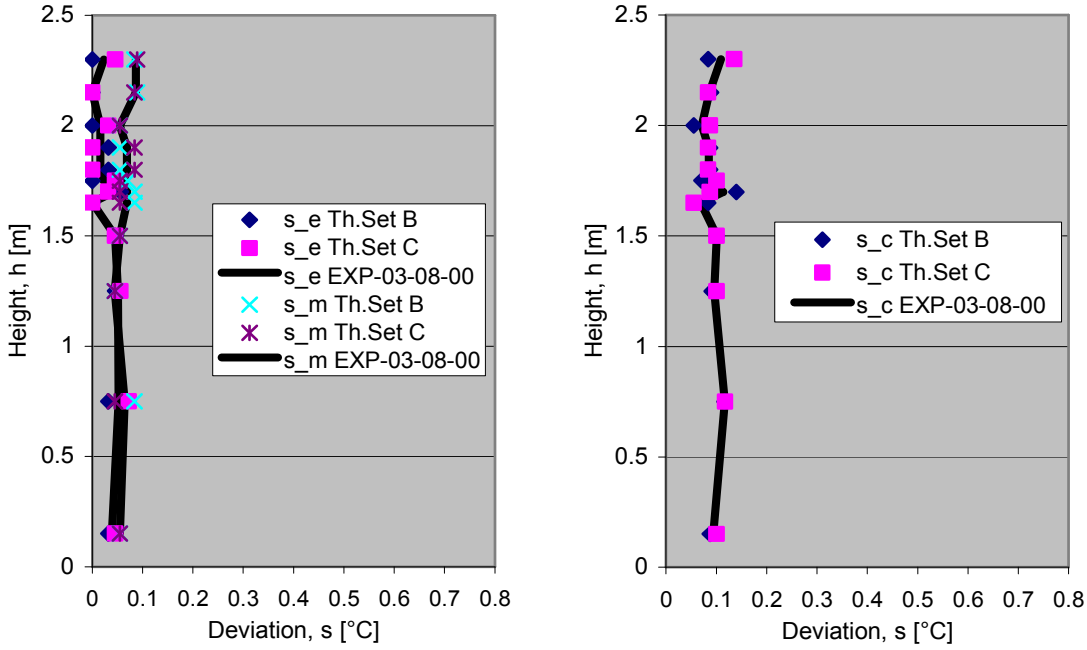

(e)

(f)

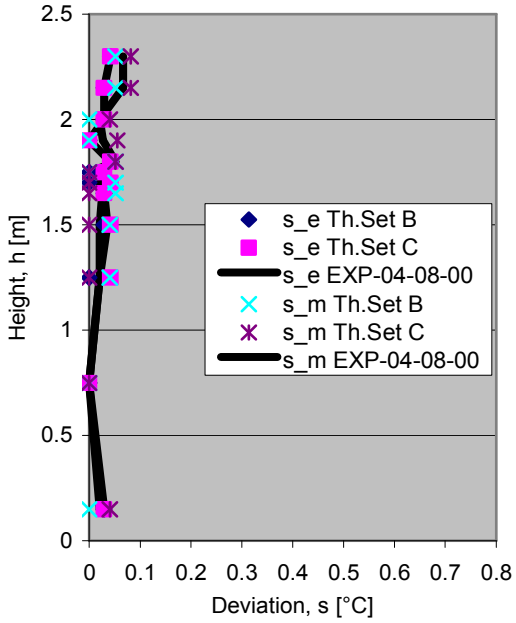

(g)

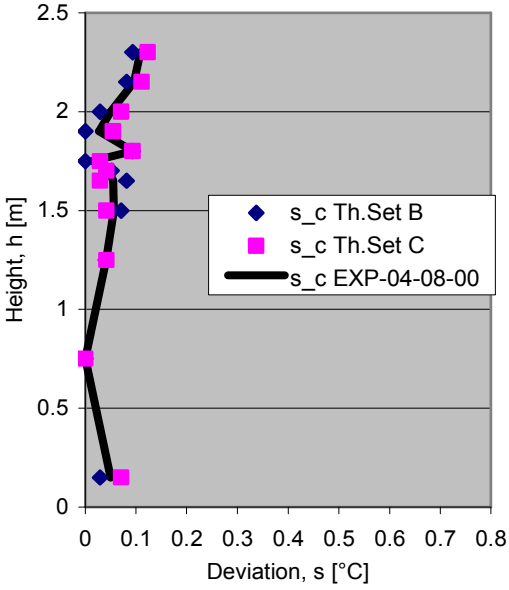

(h)

Figure 1.3: Error deviations for high and low frequencies obtained in the last two rows (1/3 of the time interval towards the end of the run) form the experimental cases of (a)&(b) EXP01, (c)&(d) EXP02, (e)&(f) EXP03 and (g)&(h) EXP04.

The flow variation is analysed here in the region in front of hot air supply jet as it follows below,

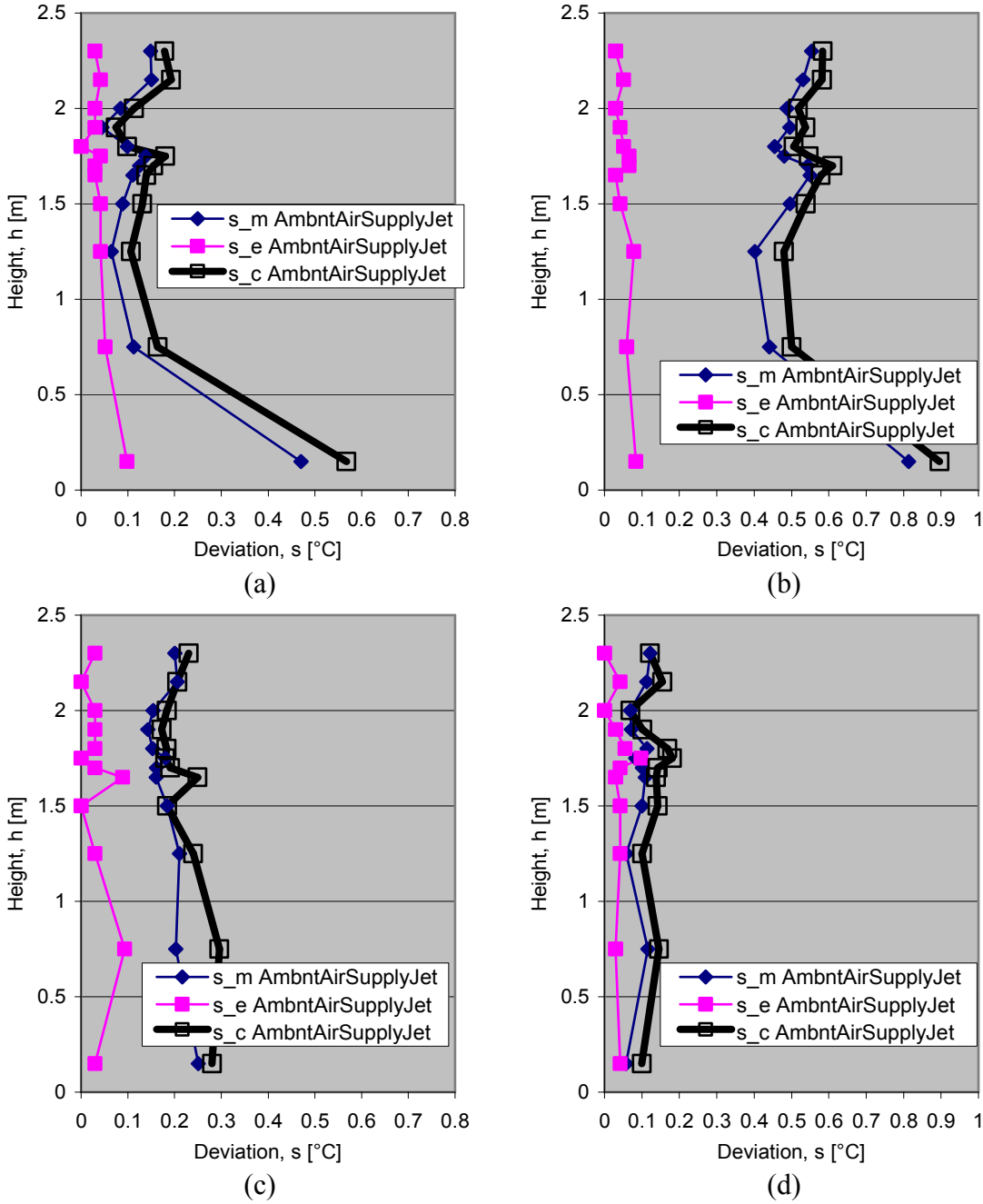

Figure 1.4: Error deviations for the high and low frequencies obtained in the region of the ambient air supply jet from the experimental cases of (a) EXP01, (b) EXP02, (c) EXP03 and (d) EXP04.

The flow variation is analysed here in the region below the hot air supply jet as it follows below,

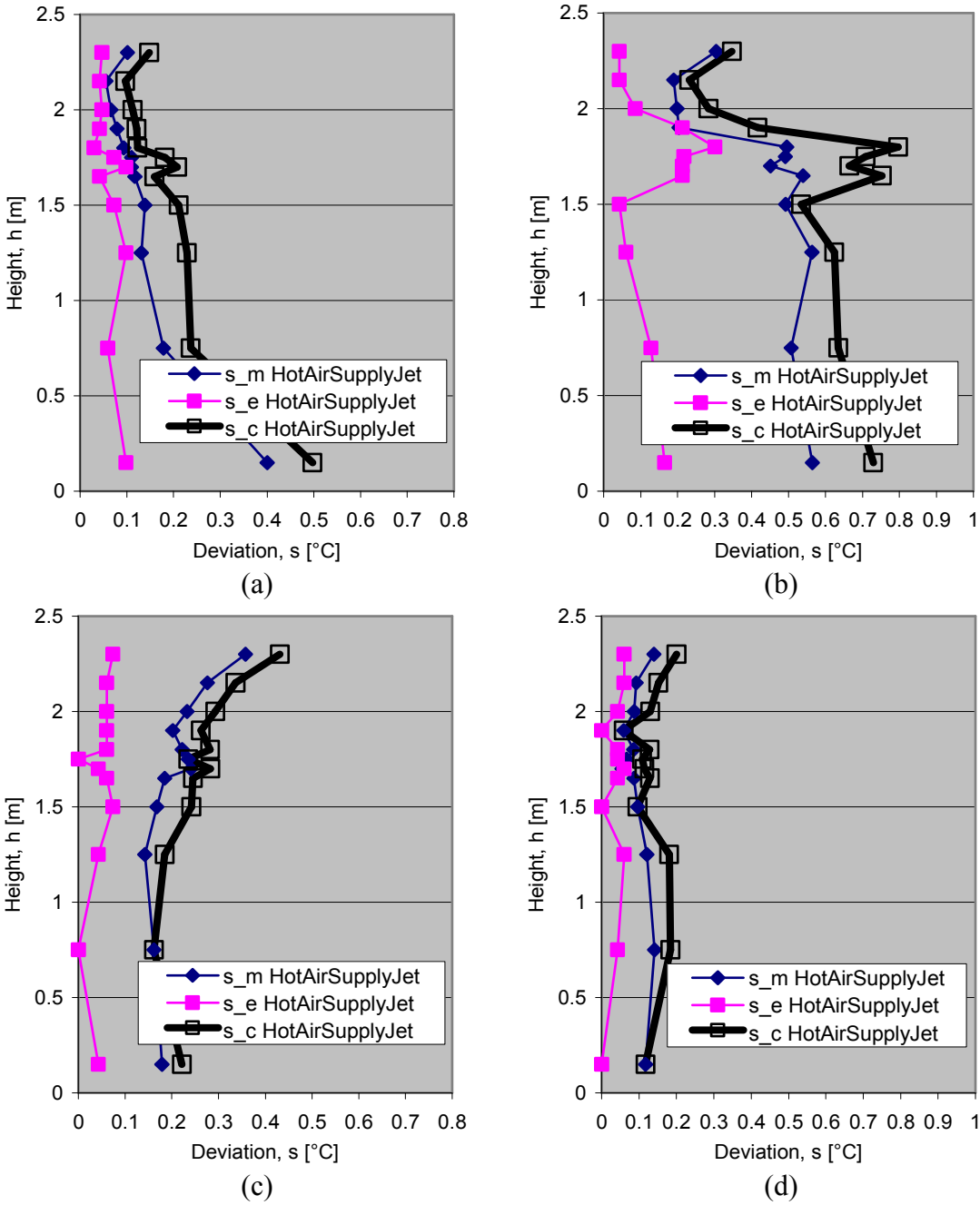

Figure 1.5: Error deviations for high and low frequencies obtained in the region of the hot air supply jet from the experimental cases of (a) EXP01, (b) EXP02, (c) EXP03 and (d) EXP04.

The deviation of the mean between the temperature distributions below the hot air supply is higher than any other place in the environmental chamber. This is observed in both experiments, where the hot air supply jet was used. The statistical analysis of the deviation of the hot air supply jet is also another proof of the changes in the flow field that occur at different locations in the chamber during the experiment with high mixed flow cases.

The statistical properties of each experimental case are included in Table 1.1 for the entire range of measurements,

Name	Instrument	N_e	σ_e	cl_e	N_m	σ_m	cl_m
EXP01-08-00	Th.Set B	864	0.06	94.70%	216	0.25	95.54%
	Th.Set C	864	0.06	95.61%	216	0.23	96.34%
EXP02-08-00	Th.Set B	864	0.07	91.58%	216	0.84	95.51%
	Th.Set C	864	0.07	96.24%	216	0.76	96.28%
EXP03-08-00	Th.Set B	864	0.04	97.12%	216	0.32	94.29%
	Th.Set C	864	0.04	95.35%	216	0.33	95.30%
EXP04-08-00	Th.Set B	864	0.03	87.41%	216	0.13	91.12%
	Th.Set C	864	0.03	93.81%	216	0.14	96.45%
	TOTAL	**6912**	**0.05**	**93.98%**	**1728**	**0.38**	**95.10%**

Table 1.1: Table showing statistical properties of experiments on mixing due to high inlet flow rates for a period of 6hours; EXP01-08-00.

The statistical properties of each experimental case are included in Table 1.2 for the last two rows of the grid,

Name	Instrument	N_e	σ_e	cl_e	N_m	σ_m	cl_m
EXP01-08-00-L2R	Th.Set B	288	0.06	94.58%	72	0.17	95.54%
	Th.Set C	288	0.05	95.61%	72	0.2	96.34%
EXP02-08-00-L2R	Th.Set B	288	0.05	95.72%	72	0.23	95.51%
	Th.Set C	288	0.04	94.43%	72	0.22	96.28%
EXP03-08-00-L2R	Th.Set B	288	0.03	94.03%	72	0.07	94.29%
	Th.Set C	288	0.05	98.22%	72	0.06	95.30%
EXP04-08-00-L2R	Th.Set B	288	0.02	88.77%	72	0.03	91.12%
	Th.Set C	288	0.03	91.66%	72	0.04	96.45%
	TOTAL	**2304**	**0.04**	**94.13%**	**576**	**0.13**	**95.10%**

Table 1.2: Table showing statistical properties of experiments on mixing due to high inlet flow rates in the region of the last two rows for a period of 2hours; EXP01-08-00-L2R.

The statistical properties of each experimental case are included in Table 1.3 for the region of the ambient air supply jet,

Name	Instrument	N_e	σ_e	cl_e	N_m	σ_m	cl_m
EXP01-08-00-AJ	Th.Set B&C	288	0.05	96.77%	72	0.2	95.51%
EXP02-08-00-AJ	Th.Set B&C	288	0.06	95.72%	72	0.53	93.91%
EXP03-08-00-AJ	Th.Set B&C	288	0.03	96.11%	72	0.2	95.12%
EXP04-08-00-AJ	Th.Set B&C	288	0.02	91.20%	72	0.09	93.15%
	TOTAL	**1152**	**0.04**	**94.95%**	**288**	**0.26**	**94.42%**

Table 1.3: Table showing statistical properties of experiments on mixing due to high inlet flow rates in the region of ambient air supply jet for a period of 1hour; EXP01-08-00-AJ.

The statistical properties of each experimental case are included in Table 1.4 for the region below the hot air supply jet,

Name	Instrument	N_e	σ_e	cl_e	N_m	σ_m	cl_m
EXP01-08-00-HJ	Th.Set B&C	288	0.07	95.19%	72	0.19	95.57%
EXP02-08-00-HJ	Th.Set B&C	288	0.14	88.45%	72	0.48	94.36%
EXP03-08-00-HJ	Th.Set B&C	288	0.03	90.64%	72	0.2	90.52%
EXP04-08-00-HJ	Th.Set B&C	288	0.02	92.67%	72	0.11	95.66%
	TOTAL	**1152**	**0.07**	**91.74%**	**288**	**0.25**	**94.03%**

Table 1.4: Table showing statistical properties of experiments on mixing due to high inlet flow rates in the region of hot air supply jet for a period of 1hour; EXP01-08-00-HJ.

1.3.2 Heat gains from solar radiation - EXP-14-11-00

The results from the experiment of the effect of solar radiation show a difference of 1°C in the hot air zone and 2°C in the cold air zone as well as a change in the temperature distribution that occurred due to sun fall from the reduction in the temperature in the hot air zone that is of the order of 0.5°C. This is shown in Figure 1.6 below,

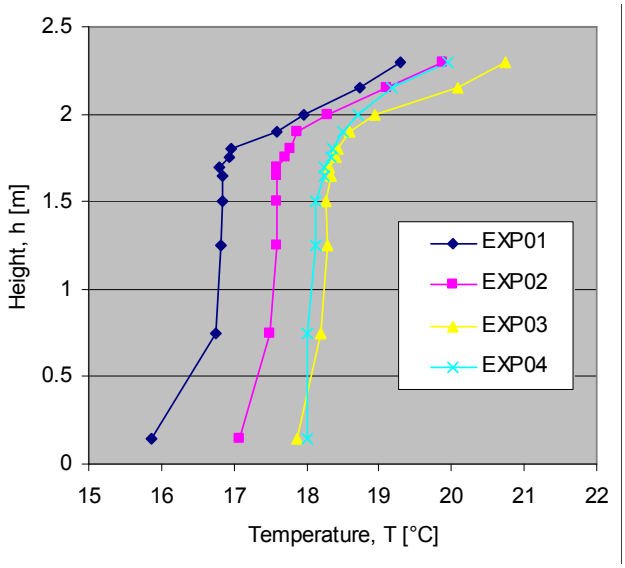

Figure 1.6: Temperature variation with height affected by external solar radiation and other heat losses while the same inlet conditions are maintained throughout the experiment; Th.Set B&C (EXP-14-11-00).

The experimental cases EXP01 and EXP04 are carried out at the start and the end of the experiment. The experimental cases EXP03 and EXP04 approximately 1hour apart from Th.Set B&C, and four samples are taken every approximately 15min in 2-min intervals. The deviation levels obtained for the case of solar heat gains change with respect to the energy levels. The same levels are obtained from the two Th.Sets. The deviations are grouped together in Figure 1.7 to make the comparison easier,

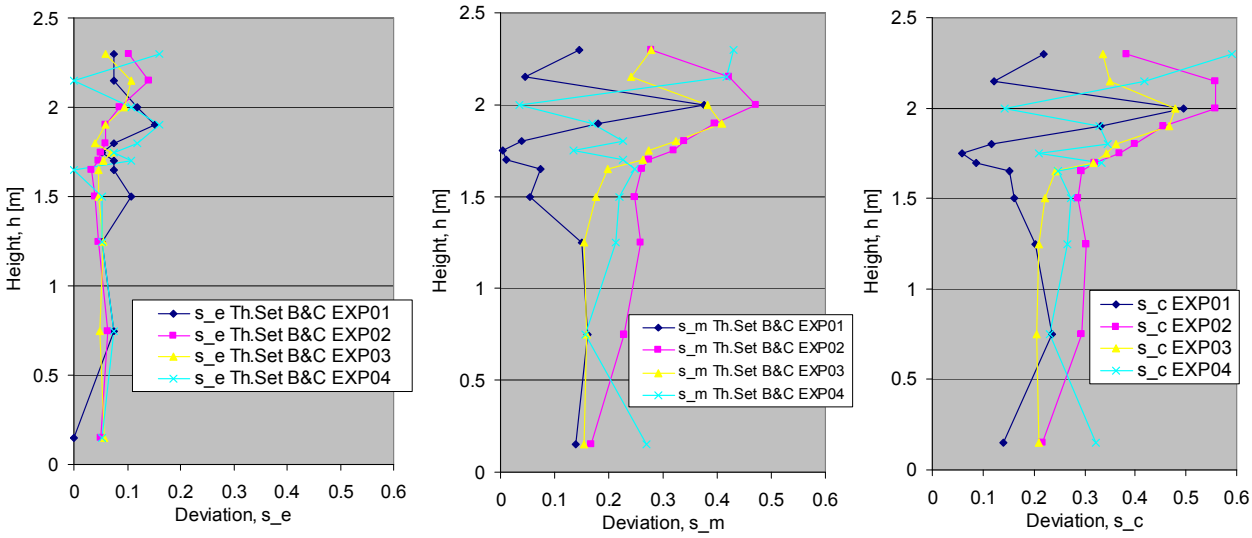

(a) (b) (d)

Figure 1.7: Deviations across height as the measurements increase in time, for i(=1,2,…,12)×n. In (a), deviation of means from the 2-min samples every 15-min intervals. In (b), deviations around the mean occurring in 2-min interval from 10-sec sample-readings across room height. (Th.Set B&C EXP-14-12-00).

The deviations that are obtained from all the experimental cases are better matching in the cold air zone. However, there is a small increase in the deviations from EXP01 up to EXP03. This happens because the temperature distribution responds to the external heat source due to solar radiation. This response is more pronounced in the hot air zone due to the inflow from the hot air supply up to case EXP03. However, in the case of EXP04, the heat gains stops and the deviation decreases to the initial levels.

To obtain the rms-mean deviation, the temperature distributions with height for each sample of 12 readings from each Th.Set is integrated across the room height. This is done for each sample every 15-min intervals for each Th.Set. It can be seen form the deviations obtained by the two Th.Sets in Figure 1.8 that there is a periodical similarity in the results,

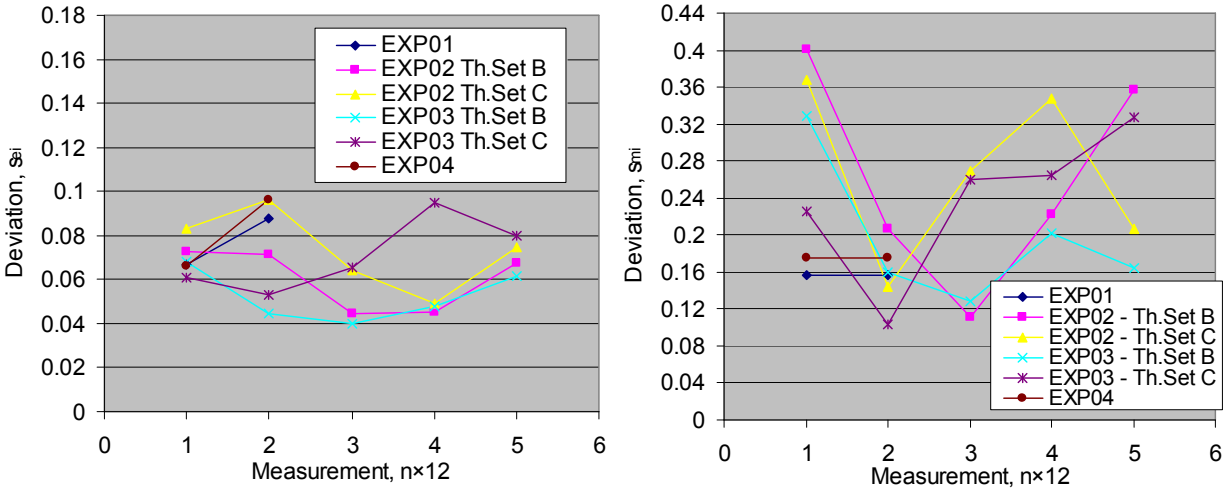

(a) (b)

Figure 1.8: In (a), deviation of error around the mean for each Th.Set and experimental time instance where i=1,2,…,5. In (b), deviation in terms of stability of the mean across height as the measurements increase in time, for i=1,2,…,5. (Th.Set B&C EXP-14-11-00).

The statistical properties are of this experiment are included in Table 1.5 for each experimental case,

Name	Instrument	N_e	σ_e	cl_e	N_m	σ_m	cl_m
EXP01-14-11-00	Th.Set B	96	0.07	91.76%	24	0.16	86.96%
	Th.Set C	96	0.1	92.65%	24		
EXP02-14-11-00	Th.Set B	240	0.06	94.47%	60	0.29	92.82%
	Th.Set C	240	0.08	94.31%	60	0.29	93.15%
EXP03-14-11-00	Th.Set B	480	0.05	94.28%	120	0.21	92.91%
	Th.Set C	480	0.07	94.49%	120	0.24	92.63%
EXP04-14-11-00	Th.Set B	96	0.07	90.98%	24	0.23	87.29%
	Th.Set C	96	0.1	93.07%	24		
	TOTAL	**1824**	**0.07**	**93.25%**	**456**	**0.24**	**90.96%**
						3.18	

Table 1.5: Table showing statistical properties of experiments on heat gains due to solar radiation effects for a period of 5hours; (EXP-14-11-00).

1.3.3 Plain and deflector set-up for hot air supply- EXP-30-11-00 & EXP-1-12-00

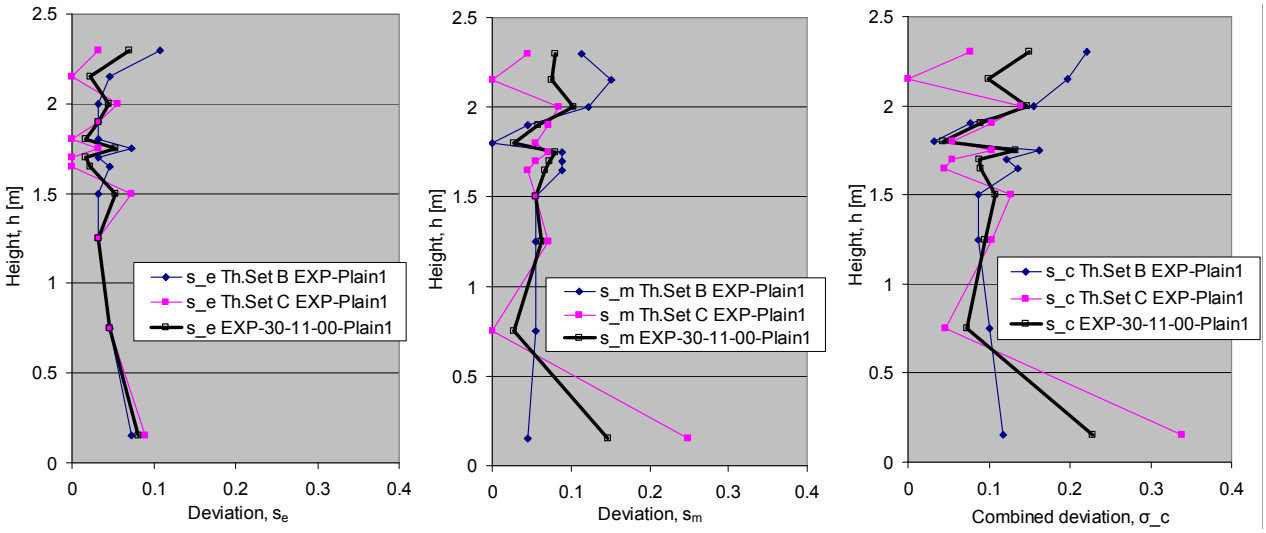

(a) (b) (c)

Figure 1.9: Deviations across height in experimental case with the plain hot air supply, as the measurements increase in time for i(=1,2,…,12)×n. In (a), deviation of error around the mean for each sample case of i=1,2,…,5. In (b), deviation in terms of stability of the mean across height as the measurements increase in time, for i=1,2,…,5; In (c), combined deviations; Th.Set B & C (EXP-30-11-00).

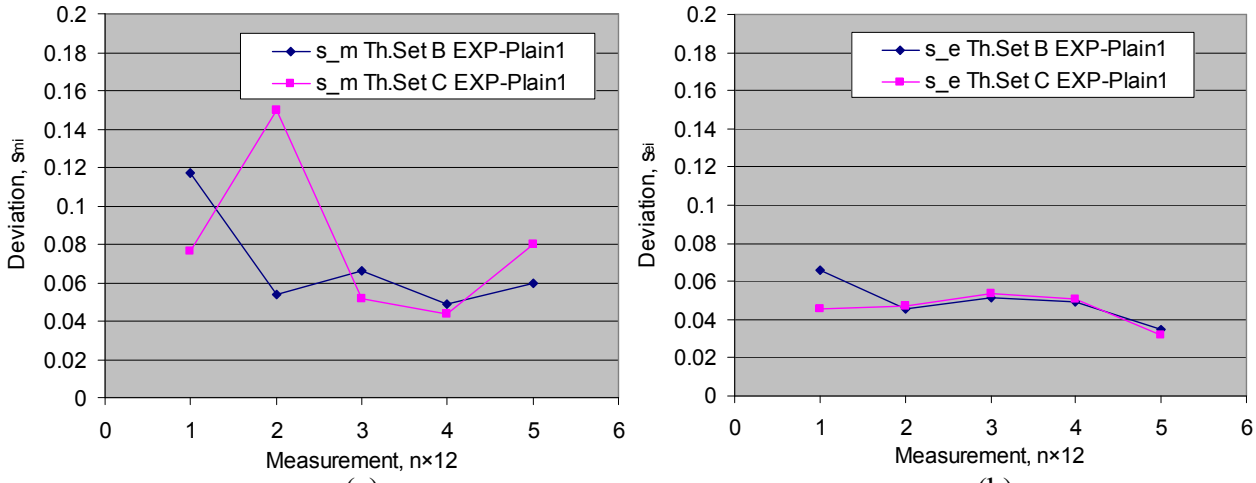

(a) (b)

Figure 1.10: In (a), deviation of error around the mean for each sample case of i=1,2,…,5. In (b), deviation in terms of stability of the mean across height as the measurements increase in time, for i=1,2,…,5.; Th.Set B & C (EXP-30-11-00).

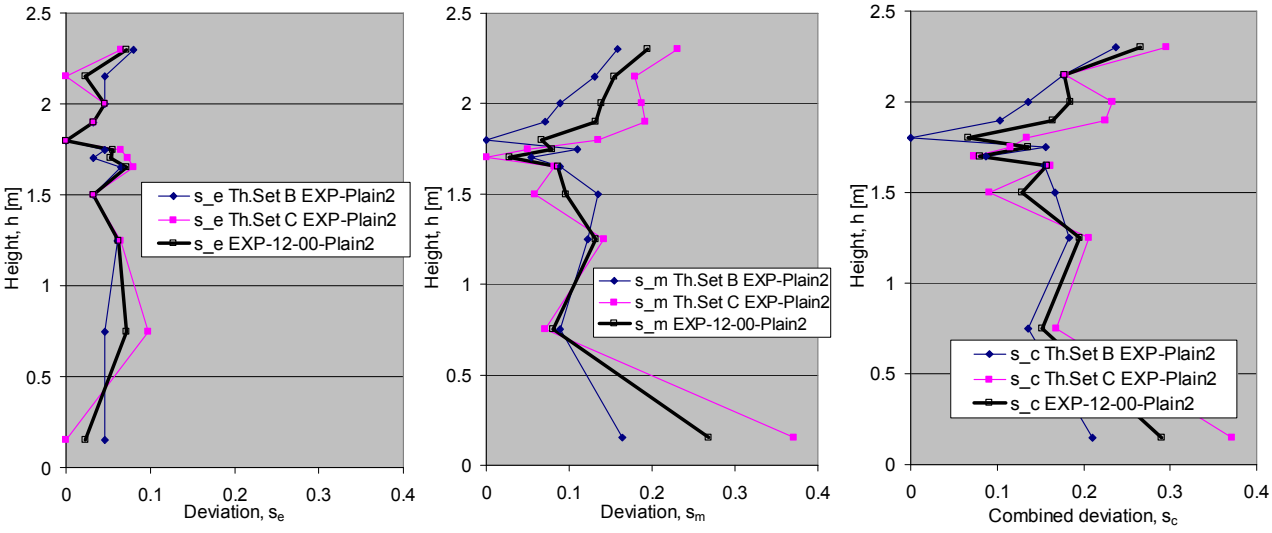

(a) (b) (c)

Figure 1.11: Deviations across height in experimental case with the plain hot air supply, as the measurements increase in time for i(=1,2,…,12)×n. In (b), deviations around the mean occurring in 2-min interval from 10-sec sample-readings across room height. In (b), deviation of means from the 2-min samples every 15-min intervals. In (c), combined deviations. Th.Set B&C (EXP-1-12-00).

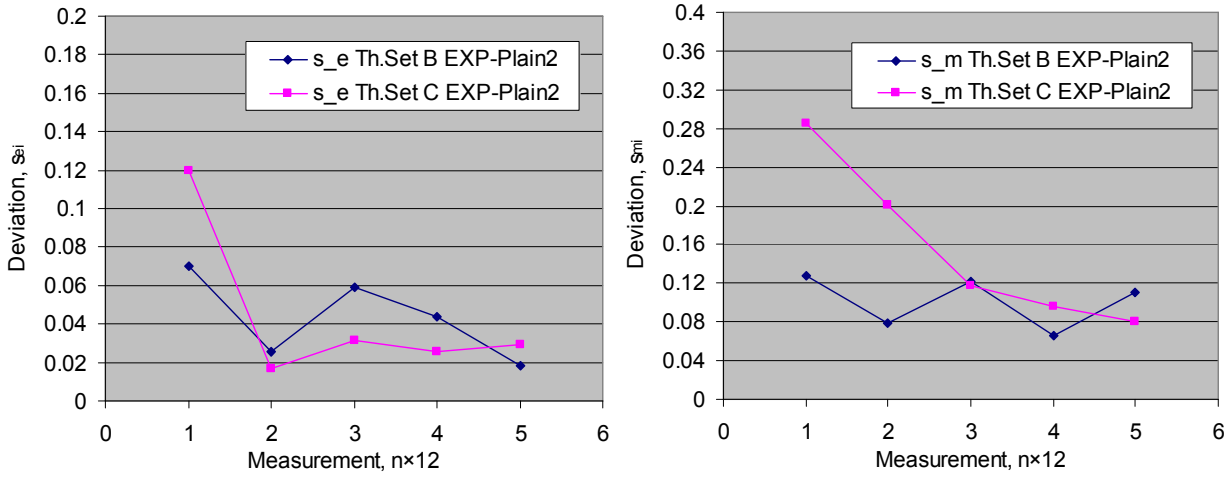

(a) (b)

Figure 1.12: In (a), deviation of error around the mean for each sample case of i=1,2,…,5. In (b), deviation in terms of stability of the mean across height as the measurements increase in time, for i=1,2,…,5. Th.Set B & C (EXP-01-11-00-Plain_Set-up).

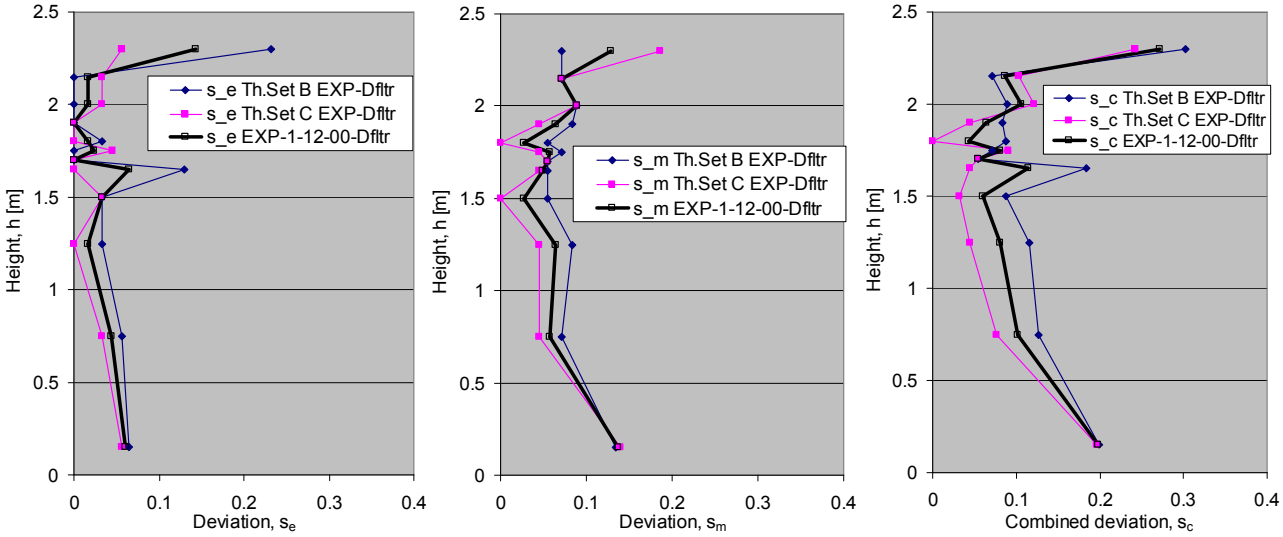

(a) (b) (c)

Figure 1.13: Deviations across height in experimental case with the deflector below the hot air supply, as the measurements increase in time for i(=1,2,…,12)×n. In (a), deviations around the mean occurring in 2-min interval from 10-sec sample-readings across room height. In (b), deviation of means from the 2-min samples every 15-min intervals. (Th.Set B&C EXP-14-12-00).

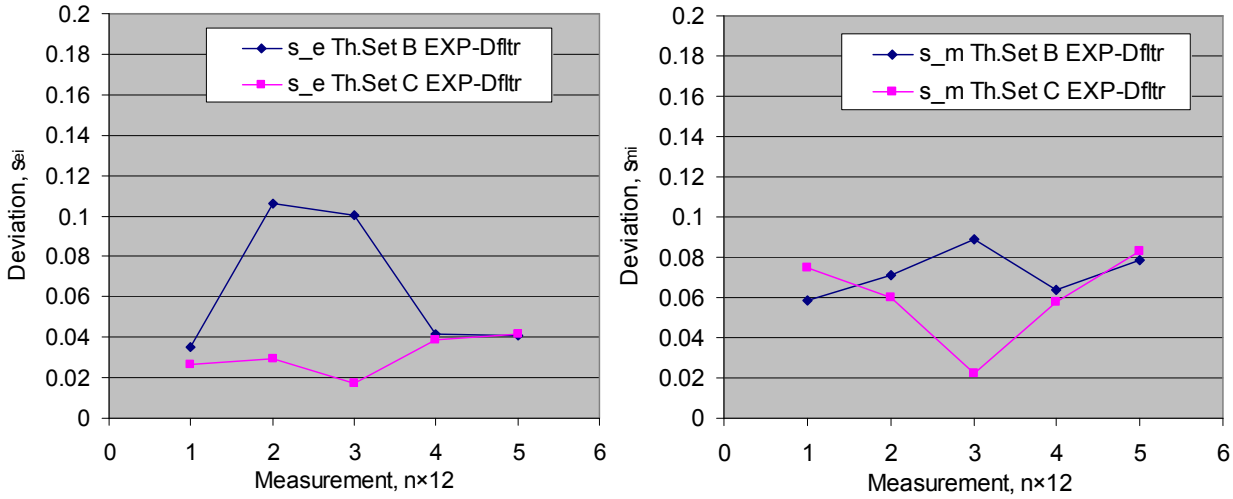

(a) (b)

Figure 1.14: In (a), deviation of error around the mean for each sample case of i=1,2,…,5. In (b), deviation in terms of stability of the mean across height as the measurements increase in time, for i=1,2,…,5. Th.Set B&C (EXP-01-11-00-Dfltr_Set-up).

Name	Instrument	N_e	σ_e	cl_e	N_m	σ_m	cl_m
EXP-30-12-00	Th.Set B	240	0.05	94.09%	60	0.07	92.96%
	Th.Set C	240	0.05	93.28%	60	0.1	92.68%
EXP-01-12-00-Plain_Set-up	Th.Set B	240	0.05	94.15%	60	0.12	92.22%
	Th.Set C	240	0.06	99.05%	60	0.18	92.22%
EXP-01-12-00-Dfltr_Set-up	Th.Set B	240	0.07	95.30%	60	0.08	92.66%
	Th.Set C	240	0.03	93.04%	60	0.08	91.89%
	TOTAL	**720**	**0.05**	**94.82%**	**360**	**0.11**	**92.44%**

Table 1.6: Table showing statistical properties of experiments with a good level of confidence for different inlet configurations.

1.3.4 High input rates - EXP-5-12-00

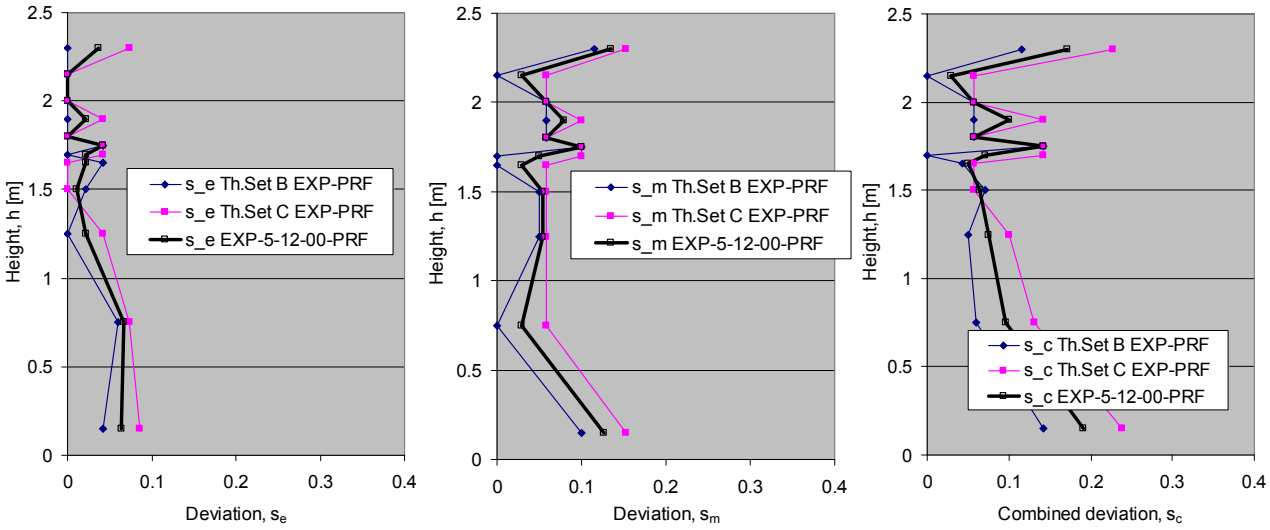

(a) (b) (c)

Figure 1.15: Case study PRF.

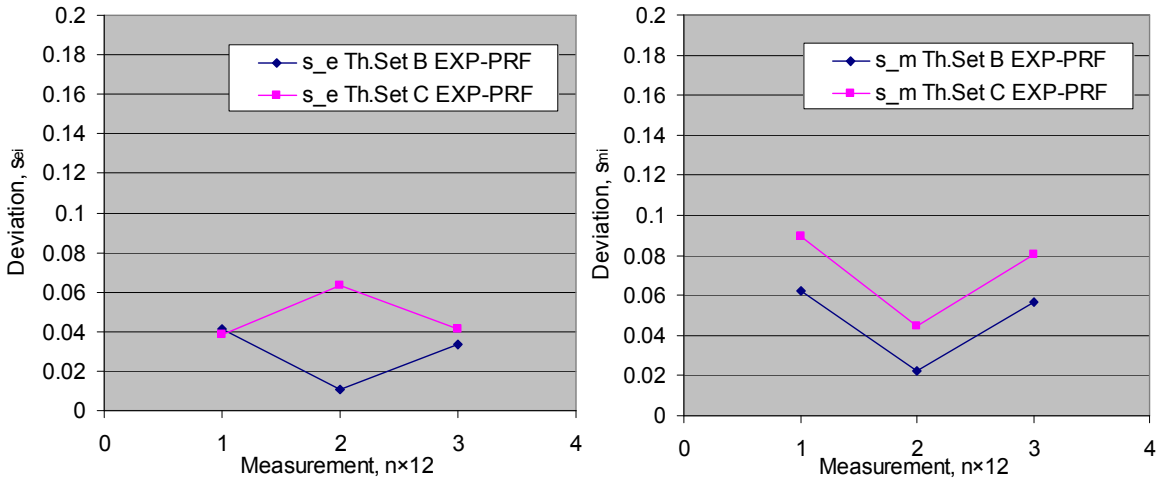

(a) (b)

Figure 1.16: Case study PRF.

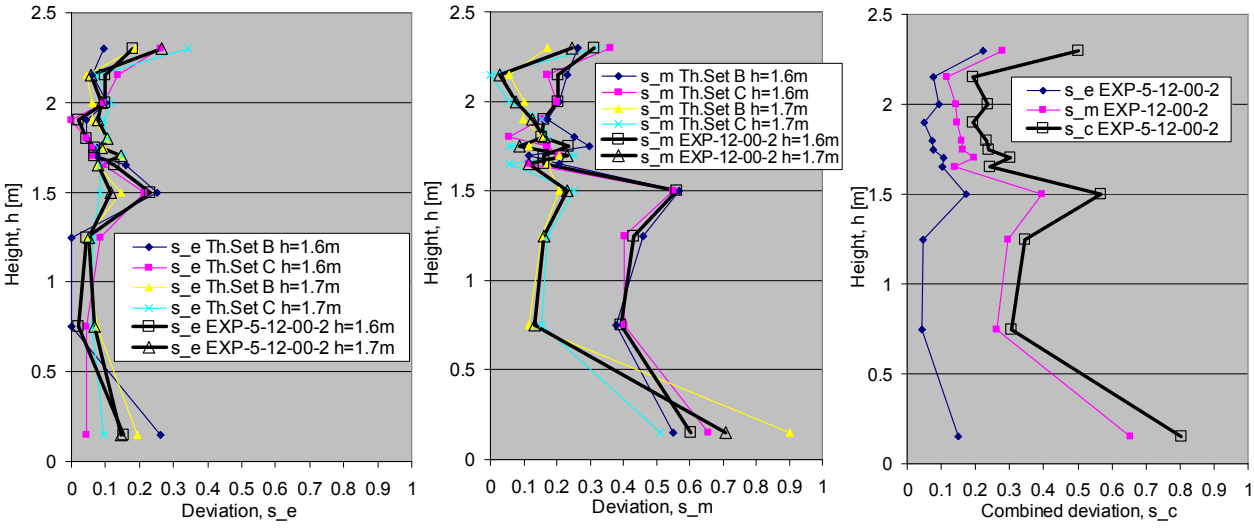

(a) (b) (c)

Figure 1.17: Case studies EXP02 and EXP03.

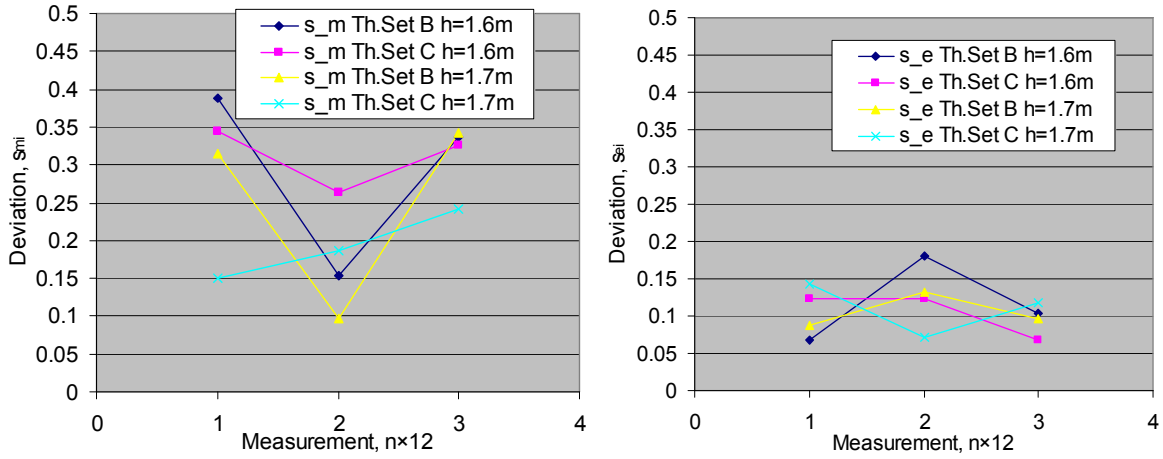

(a) (b)

Figure 1.18: Case studies EXP02 and EXP03.

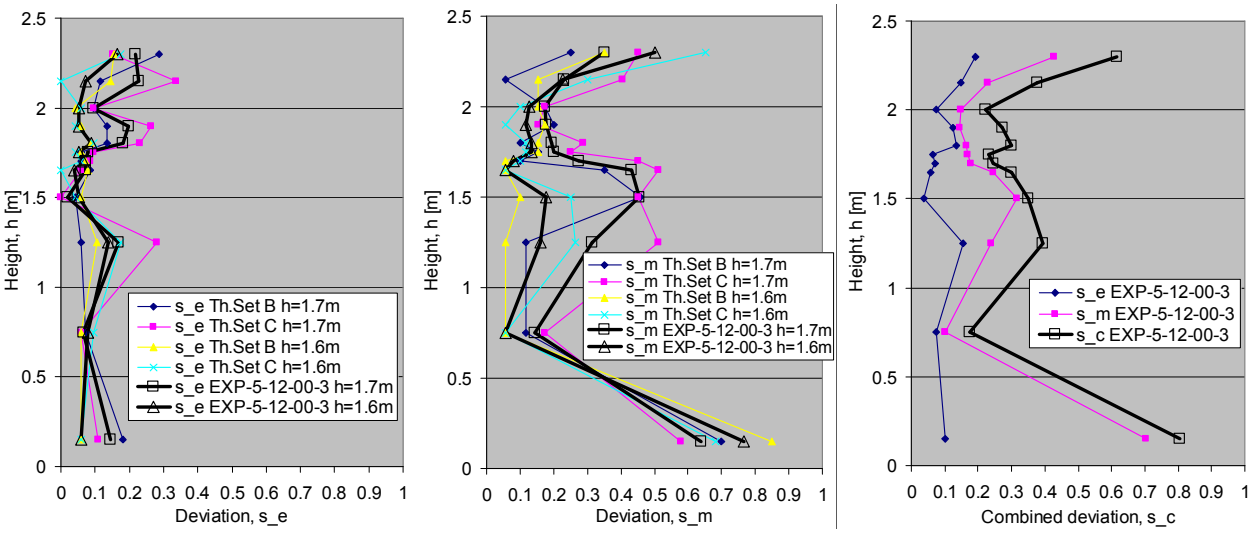

(a) (b) (c)

Figure 1.19: Case studies EXP04 and EXP05.

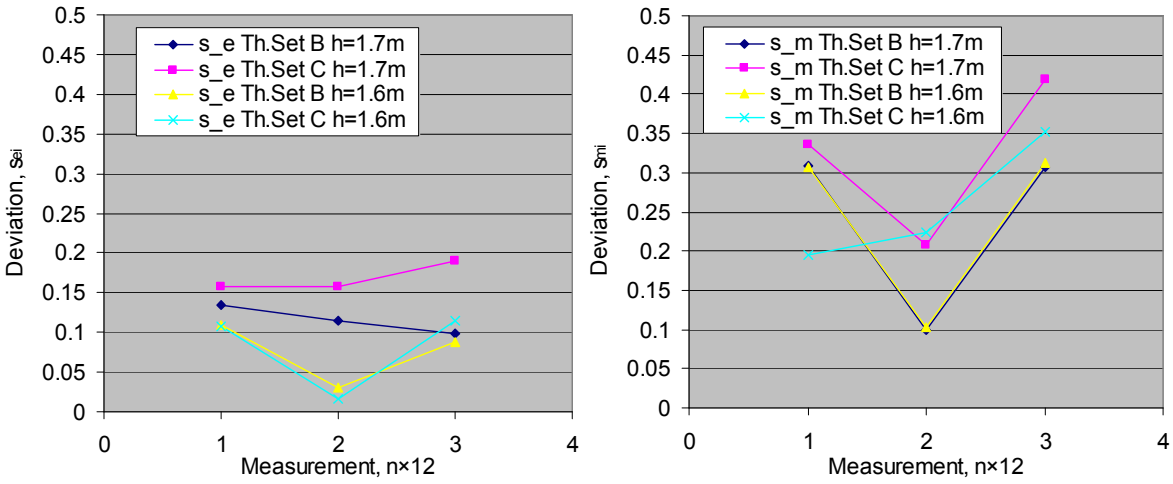

(e) (f)

Figure 1.20: In (a), deviation in terms of stability of the mean across height as the measurements increase in time, for i=1,2,…,5. In (b), deviation of error around the mean for each sample case of i=1,2,…,5; Th.Set B & C (EXP-5-12-00).

Name	Instument	N_e	σ_e	cl_e	N_m	σ_m	cl_m
EXP01-05-12-00	Th.Set B	144	0.04	91.63%	36	0.06	89.52%
	Th.Set C	144	0.06	92.15%	36	0.09	90.83%
EXP02-05-12-00-h=1.6m	Th.Set B	144	0.14	91.82%	36	0.4	89.77%
	Th.Set C	144	0.11	93.34%	36	0.41	89.21%
EXP02-05-12-00-h=1.7m	Th.Set B	144	0.11	93.06%	36	0.36	92.88%
	Th.Set C	144	0.1	95.79%	36	0.25	91.50%
EXP03-05-12-01-h=1.7m	Th.Set B	144	0.11	93.50%	36	0.33	90.74%
	Th.Set C	144	0.18	92.60%	36	0.4	90.19%
EXP03-05-12-00-h=1.6m	Th.Set B	144	0.08	94.00%	36	0.34	92.79%
	Th.Set C	144	0.1	93.11%	36	0.33	90.55%
	TOTAL	**1440**	**0.1**	**93.10%**	**360**	**0.3**	**90.80%**

Table 1.7: Table showing statistical properties of experiments for experimental cases of higher inlet velocities and slightly different extract heights.

1.3.5 Low and high input rates - EXP-8-12-00

This experiment was run from low to high input rates. The first set was obtained for very low input. The second set was obtained for higher inputs by increasing the hot air supply while the cold air supply is at the previous value. The third case is for slightly higher cold air supply increments. Finally, the fourth case is carried out for the same settings as the EXP-5-12-00.

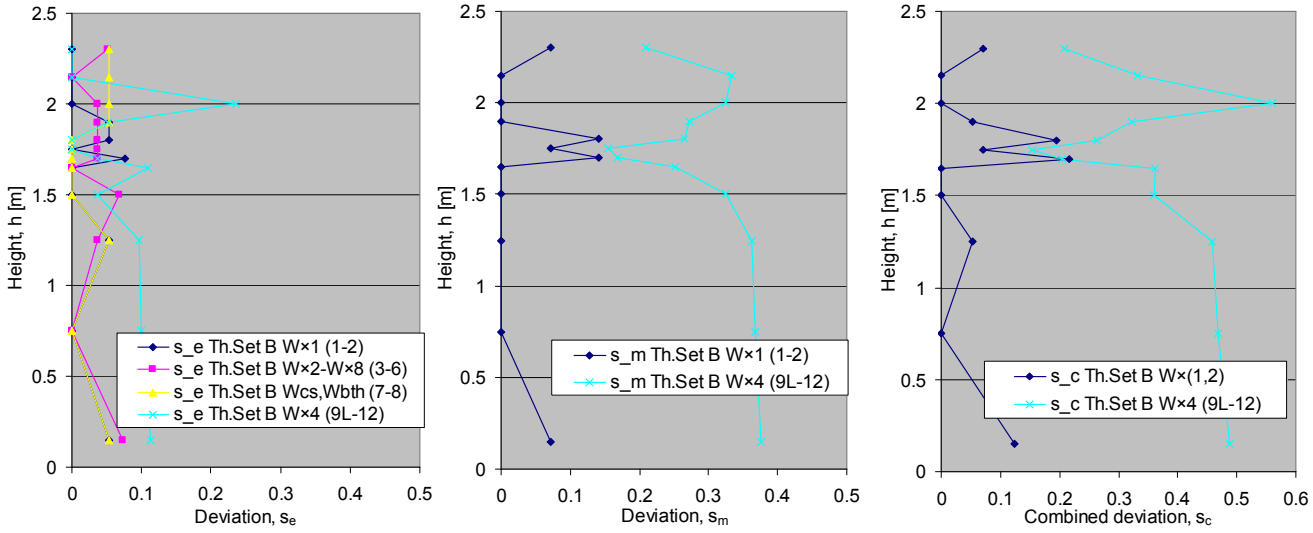

(a) (b) (c)

Figure 1.21: EXP-8-12-00.

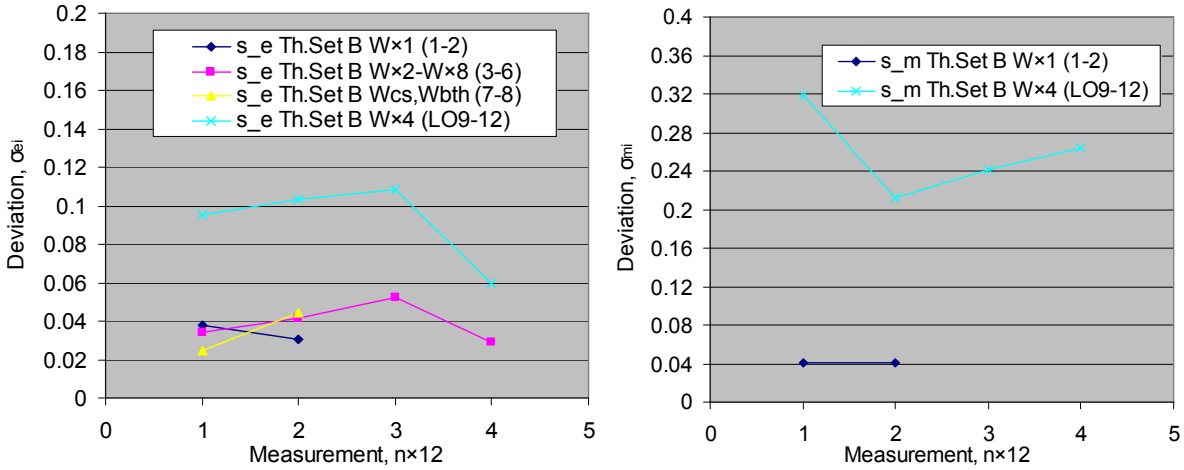

(a) (b)

Figure 1.22: In (a), deviation of error around the mean for each sample case of i=1,2,…,4. In (b), deviation in terms of stability of the mean across height as the measurements increase in time, for i=1,2,…,4. Th.Set B & C (EXP-8-12-00).

Name	Inlet Cond.	Instrument	N_e	σ_e	cl_e	N_m	σ_m	cl_m
EXP-8-12-00 Ta1 & Ta2	U=c,W×1	Th.Set B	96	0.04	89.84%	24	0.05	88.90%
EXP-8-12-00 Tb1	U=c,W×2	Th.Set B	48	0.05	89.45%	12	-	-
EXP-8-12-00 Tb2	U=c,W×4	Th.Set B	48	0.05	89.72%	12	-	-
EXP-8-12-00 Tb3	U=c,W×6	Th.Set B	48	0.06	89.79%	12	-	-
EXP-8-12-00 Tb4	U=c,W×8	Th.Set B	48	0.03	91.27%	12	-	-
EXP-8-12-00 Tc-vcold	U×2,W×8	Th.Set B	48	0.03	91.27%	12	-	-
EXP-8-12-00 Td-vboth	U×4,W×4	Th.Set B	192	0.05	89.90%	48	-	-
EXP-8-12-00	U×4,W×4	Th.Set B	192	0.1	92.42%	48	0.34	91.52%
		TOTAL	**720**	**0.05**	**90.46%**	**180**	**0.19**	**90.21%**
				0.036	1.305353		0.05	
				0.1	3.349552		0.34	

Table 1.8: Table showing statistical properties of experiments of higher inlet flow rates and slightly different extract heights; Th.Set B (EXP-8-12-00).

1.3.6 Low input rates - EXP-11-12-00

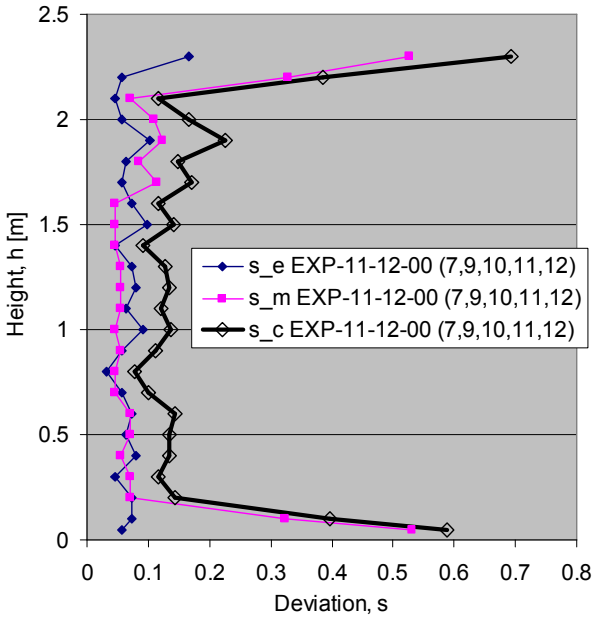

Figure 1.23: Deviation across height.

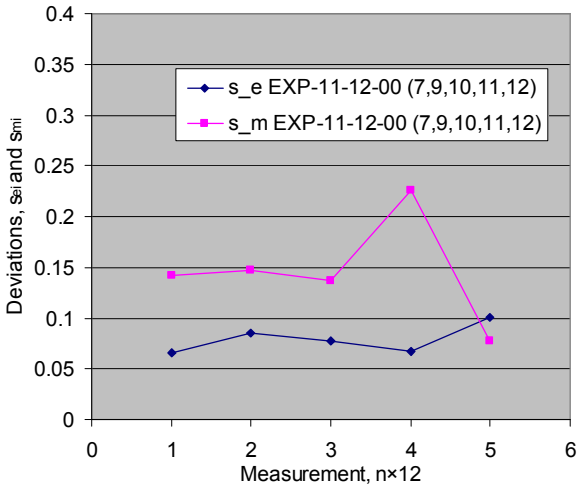

Figure 1.24: Deviation s_{mi}.

Name	Instrument	N_e	σ_e	cl_e	N_m	σ_m	cl_m
EXP-11-12-00-W1-h=1.6m (1)	Th.Set B	48	0.06	90.75%	12	-	-
	Th.Set C	48	0.04	92.99%	12	-	-
EXP-11-12-00-W2-h=1.6m (2)	Th.Set B	48	0.05	91.61%	12	-	-
	Th.Set C	48	0.01	98.80%	12	-	-
EXP-11-12-00-W3-h=1.6m (3)	Th.Set B	48	0.14	93.13%	12	-	-
	Th.Set C	48	0.07	92.56%	12	-	-
EXP-11-12-00-W4-h=1.6m (4)	Th.Set B	48	0.07	92.59%	12	-	-
	Th.Set C	48	0.03	94.04%	12	-	-
EXP-11-12-00-h=2.2m (5)	Th.Set B	48	0.05	93.23%	12	-	-
	Th.Set C	48	0.07	91.63%	12	-	-
EXP-11-12-00-h=0.8m (6)	Th.Set B	48	0.07	92.49%	12	-	-
	Th.Set C	48	0.07	92.26%	12	-	-
EXP-11-12-00-h=1.6m-BWall (8)	Th.Set B	48	0.07	91.88%	12	-	-
	Th.Set C	48	0.03	92.85%	12	-	-
EXP-11-12-00-h=1.6m AllWalls (7,9,10,11,12)	Th.Set B	240	0.08	92.99%	60	0.17	94.52%
	Th.Set C	240	0.07	94.55%	60	0.13	95.19%
EXP-11-12-00-re-check-Bwall	Th.Set B	48	0.17	95.43%	12	-	-
	Th.Set C	48	0.04	97.61%	12	-	-
	TOTAL	**1200**	**0.07**	**93.16%**	**300**	**0.15**	**94.86%**
			0.07	2.09369		0.15	

Table 1.9: Statistical properties of experiment for low inlet velocity in the environmental chamber. The statistical properties obtained from Th.Set B are from middle to ceiling. The statistical properties obtained from Th.Set C are from floor to middle; (EXP-11-12-00).

1.4 DISCUSSION

By the analysis of the calibration tests that were carried out previously, it was shown that 4 single readings are needed to get a range of accuracy equal to ±0.1°C and a deviation of σ_e=0.05.

The results that are obtained from multiple measurements showed that the error is slightly higher than the thermocouple accuracy. Depending on the inlet parameters, there is a correlation between the deviation of the error, σ_e, at the instance of the measurement and between the deviation of the mean, σ_m, from different measurements. This is depicted by the histogram in Figure 1.25,

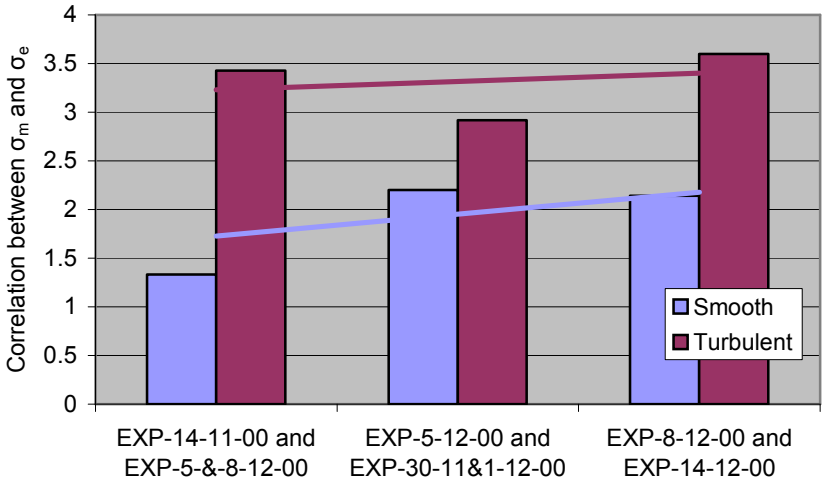

Figure 1.25: The correlation between the σ_m and σ_e for low and high input flow rates is consistent for stratified flow cases.

1.4.1 Signal description

The average magnitude of the oscillations that occur in stratified flows in buildings can be obtained by looking at the graphs of the average deviations for each experimental case. This is done first by looking at the average s_e obtained for each time-instance *i*, for which a sinusoidal function could be fitted through the points that is of the form given below,

$$f\{n,T\} = B + A\sin\left(\frac{n}{c}T\right) \tag{1.9}$$

where *n* is the measurement instance, *T* is the time period between two measurements, *B* is the offset of the function, while *c* is a constant and *A* is the amplitude.

The frequencies form the temperature oscillations are a function of the amplitude. The stronger the oscillations, the higher the amplitude of the signal. The amplitude of the signal is associated with the inlet flow rate. High flow rates correspond to larger oscillations of which the amplitude is defined by the deviation of the high and low frequencies. The higher frequencies are filtered over a period of 5-10sec.

The Gaussian filter smoothes out the data and gives a generally good idea of the signal in cases where there is not enough data to plot a perfect Gaussian distribution. There are cases where the edges of the temperature distribution are affected by the HS and CS. This leads to deviations form the straight line of the normal probability distribution. For cases that there is a strong thermal stratification, which occurs here with high inlet flow rates, the main distribution of the deviation occurs at three locations. This is below the ceiling, because of the wake of the hot air supply. Above the floor, because of the wake

of the cold air supply. Finally, up to a 1/2-room height at the interface, where the flapping motion of the interface is encountered, while the air mixes in the hot air layer and the cold air layer due to the high flow rates not concealing any considerable changes in the temperature.

A dynamical excitation is observed in the cold and hot air layers due to the hot and cold air inflow. Between the two layers there is a thinner interfacial layer. This can be inferred from the deviation of the values in that region. The dynamical excitation changes with higher inlet velocity and this can be described by the Struhal number. This is around 0.2 for low velocity flows. The Struhal number, *St*, is defined as,

$$St = \frac{fD}{u} \tag{1.10}$$

here u is the average horizontal velocity which is dependant on the inlet velocity, f is the frequency of the oscillations which is the reciprocal of 900, in most of the cases here, and D is the hydraulic diameter which is equal to 4.

1.5 SUMMARY

It can be understood from the analysis of the error deviations with different inlet flow rates that the frequency modes that occur in buildings are small enough and hence steady-state simulations will describe well enough the entire system.

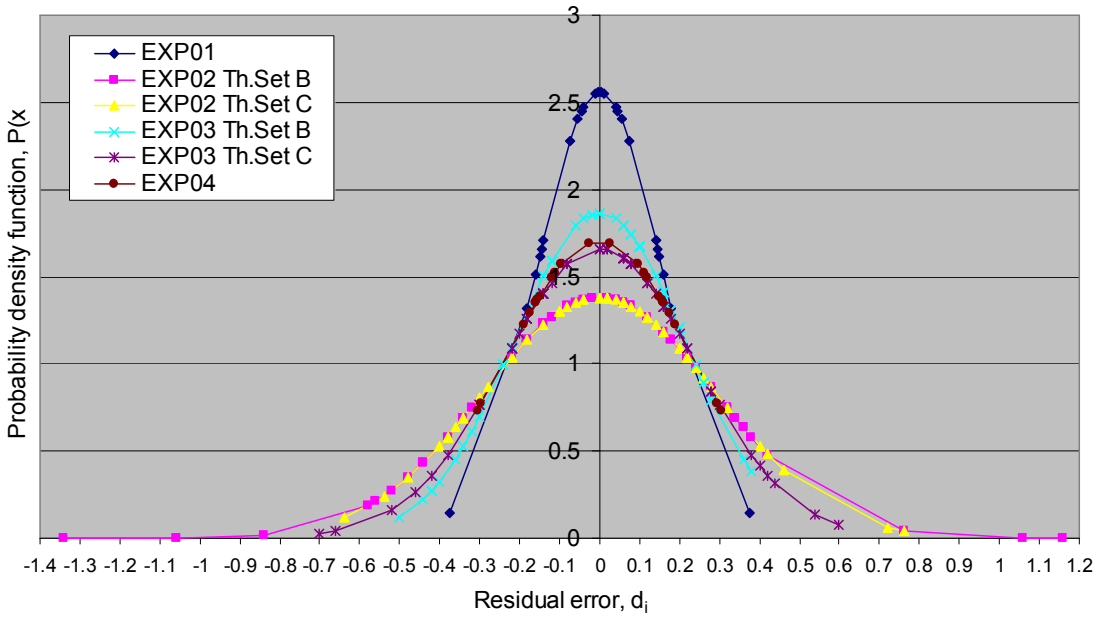

(a)

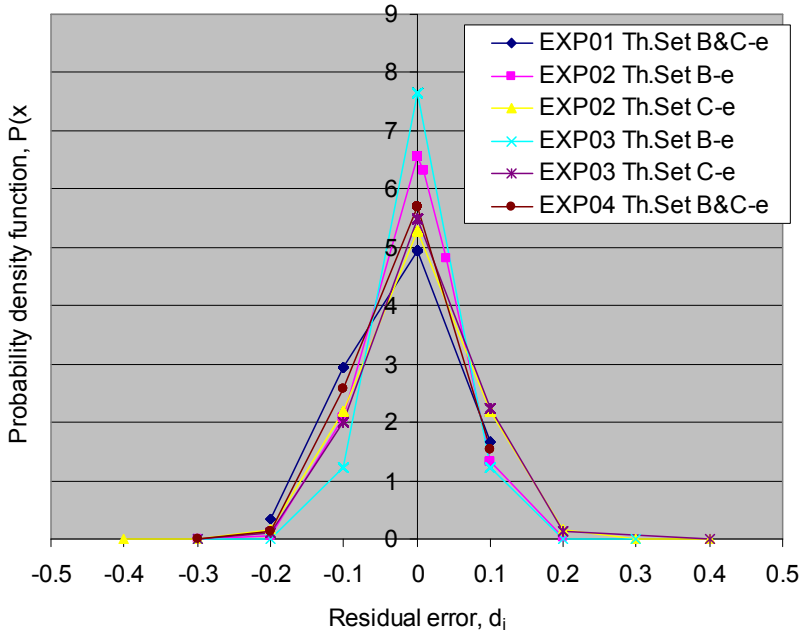

(b)

Figure 1.26: In (a), normal distributions of the mean values. In (b), normal distributions of the higher frequencies; (Th.Set EXP-14-11-00).

The probability distribution of the error of the mean values in (a) shows that a ±0.4°C error margin can be achieved for all experimental tests.

The distribution of the higher frequencies in (b) is very accurate which can be impaired from the shape of triangular distribution and is symmetric in most of the cases. The slight variation of the values is because of the increased accuracy from the 2dp.-calibration. The values are still very close to the nominal values of the prescribed precision error.

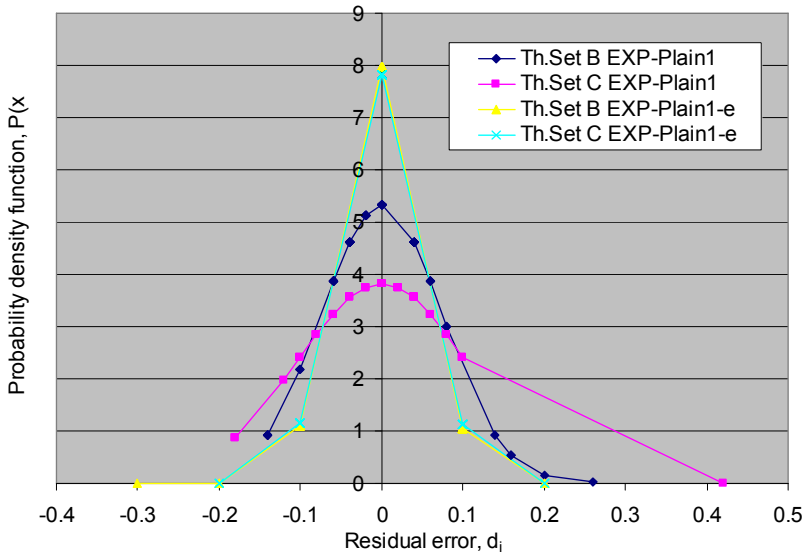

Figure 1.27: Normal distribution of low and high frequencies for Th.Set B&C EXP-30-11-00.

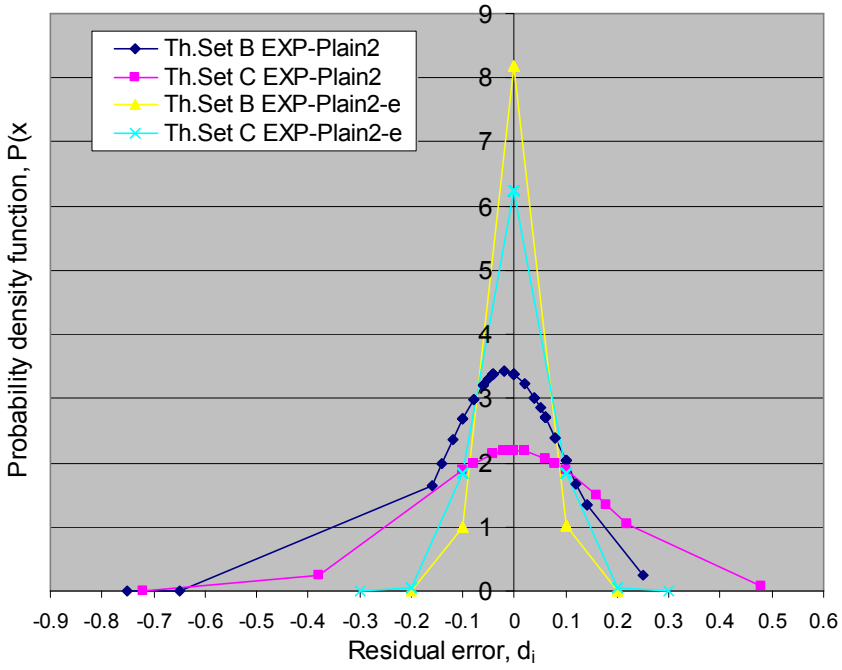

Figure 1.28: Normal distribution of low and high frequencies for Th.Set B&C EXP-01-12-00.

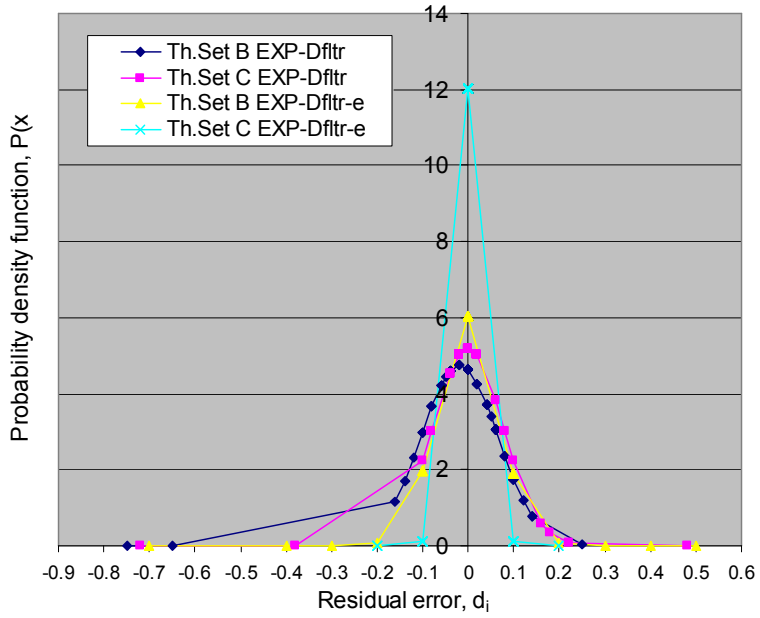

Figure 1.29: Normal distribution of low and high frequencies for Th.Set B&C EXP-01-12-00.

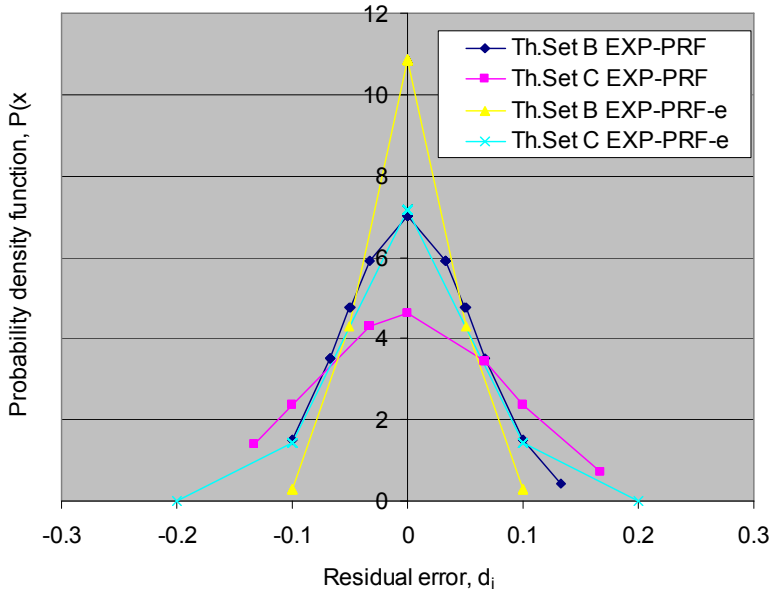

Figure 1.30: Normal distribution of low and high frequencies for Th.Set B&C EXP-05-12-00-PRF.

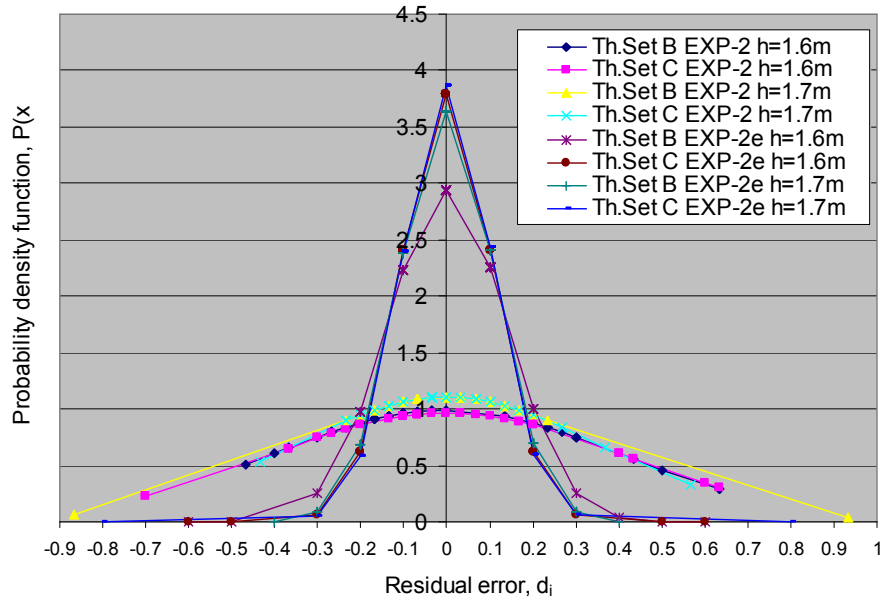

Figure 1.31: Normal distribution of low and high frequencies for Th.Set B&C EXP-05-12-00-2.

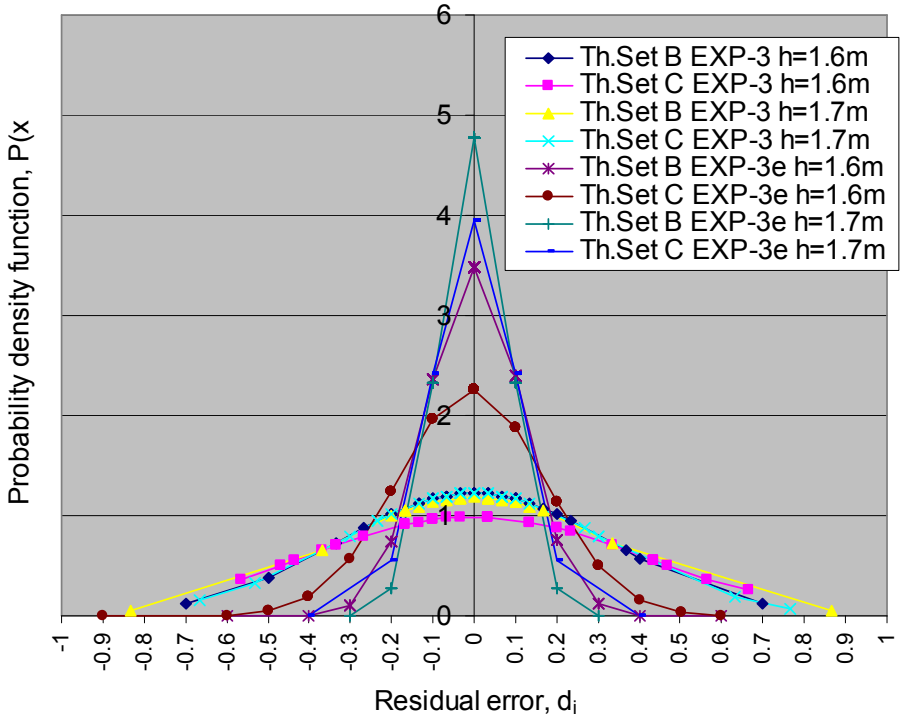

Figure 1.32: Normal distribution of low and high frequencies for Th.Set B&C EXP-05-12-00-3.

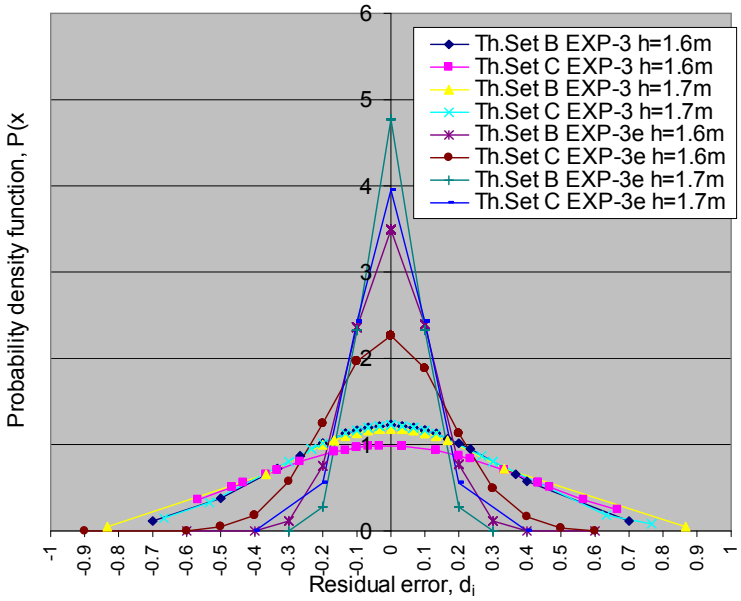

Figure 1.33:

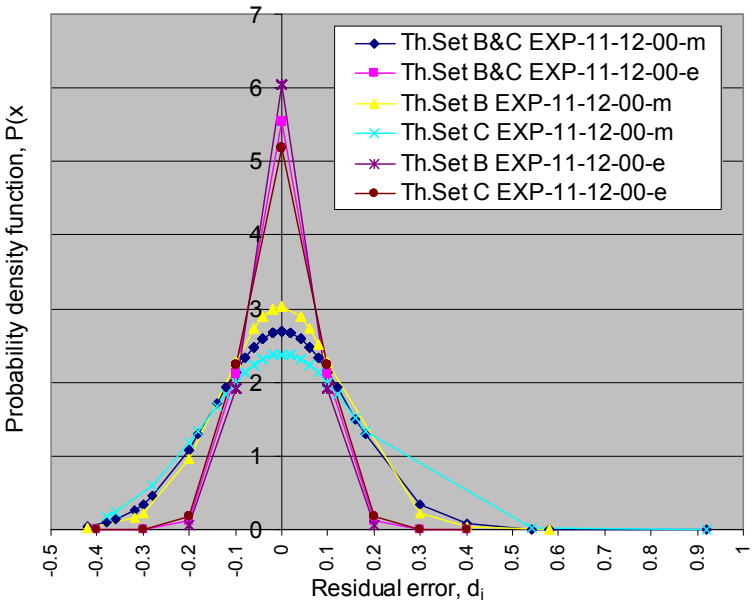

Figure 1.34:

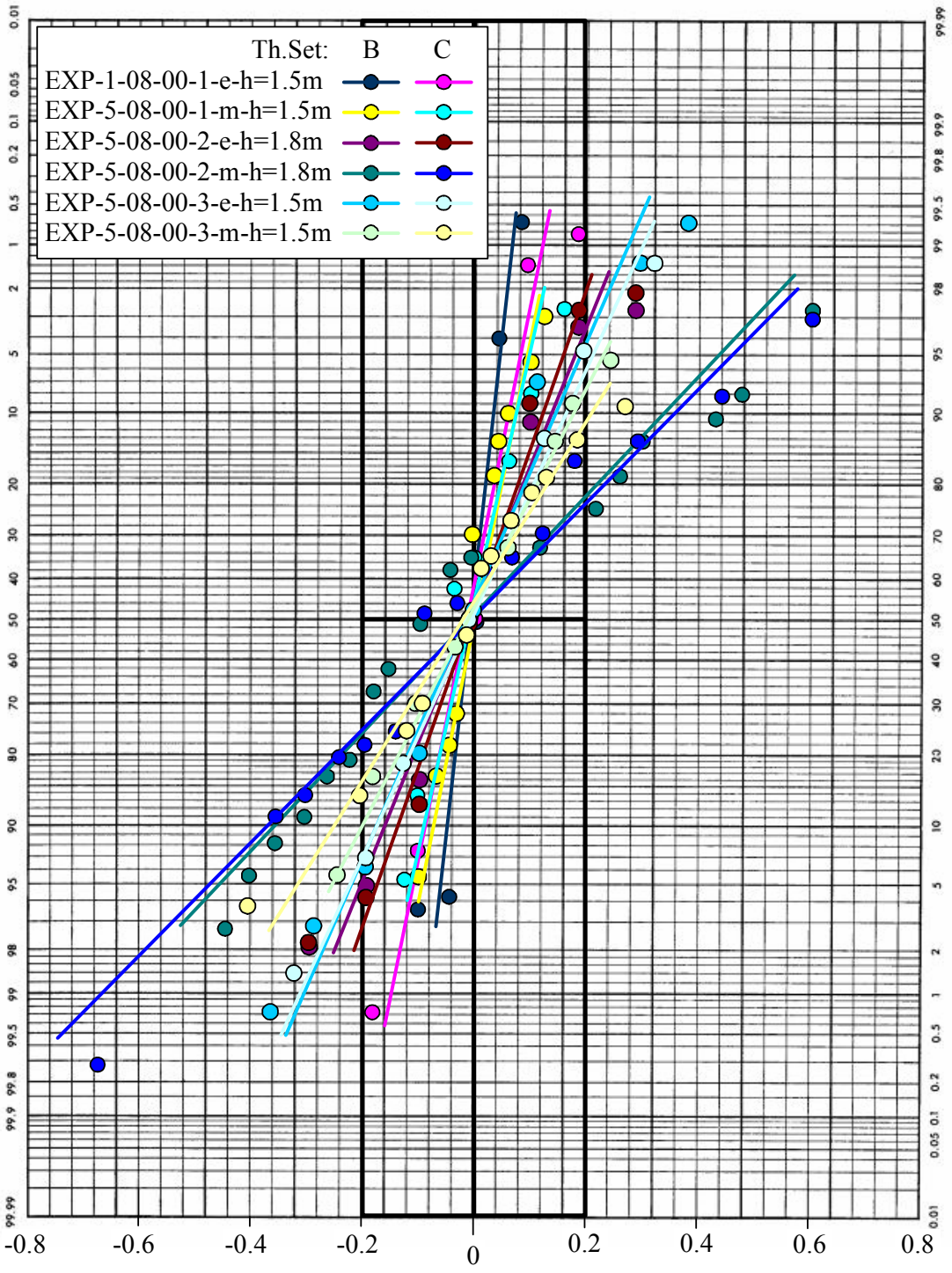
Th.Set: B C
EXP-1-08-00-1-e-h=1.5m
EXP-5-08-00-1-m-h=1.5m
EXP-5-08-00-2-e-h=1.8m
EXP-5-08-00-2-m-h=1.8m
EXP-5-08-00-3-e-h=1.5m
EXP-5-08-00-3-m-h=1.5m
-0.8
-0.6
-0.4
-0.2
0
0.2
0.4
0.6
0.8

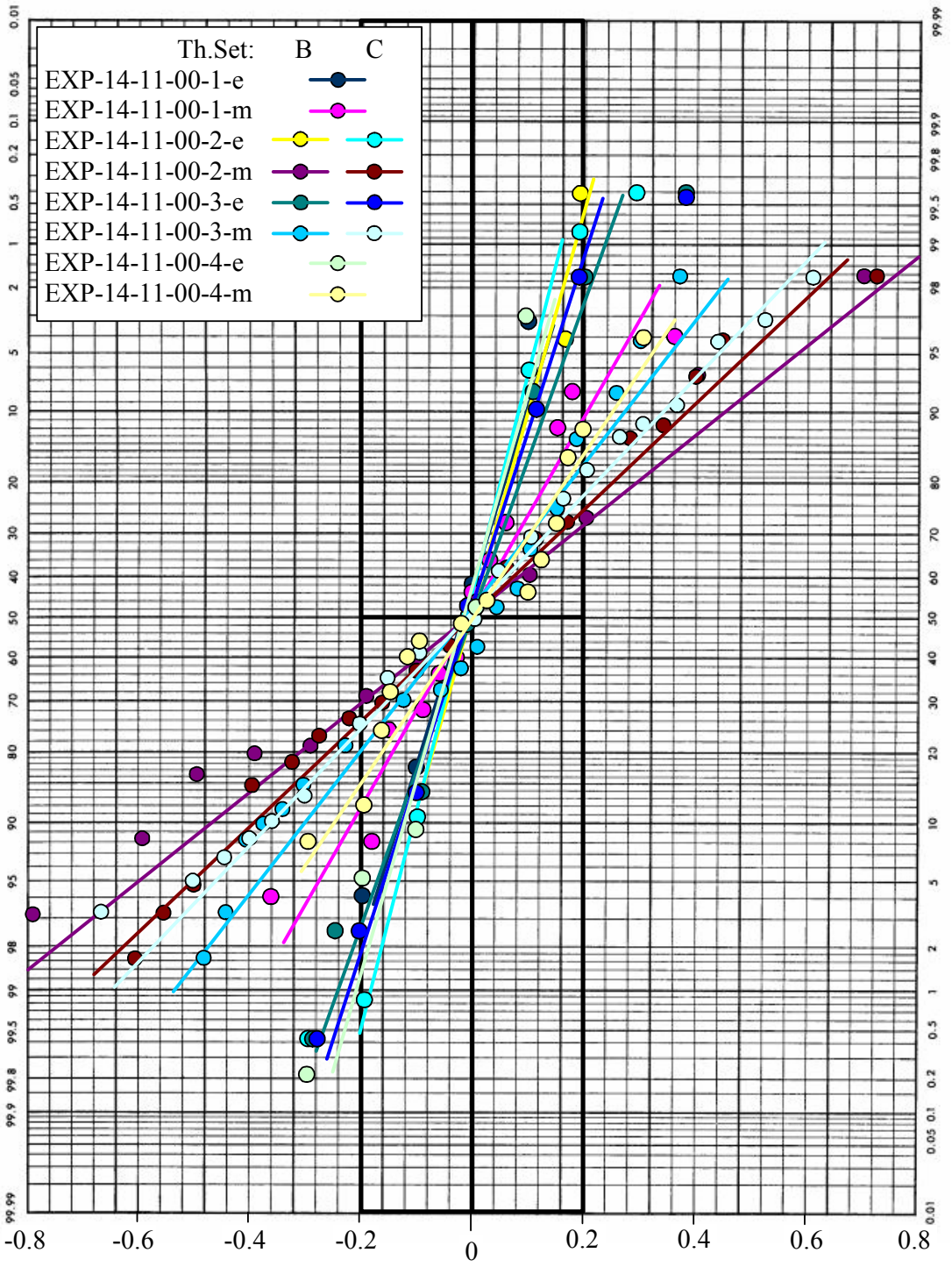

Figure 1.35: Probability check showing that the results follow a normal probability distribution; Th.Set B&C EXP-14-11-00.

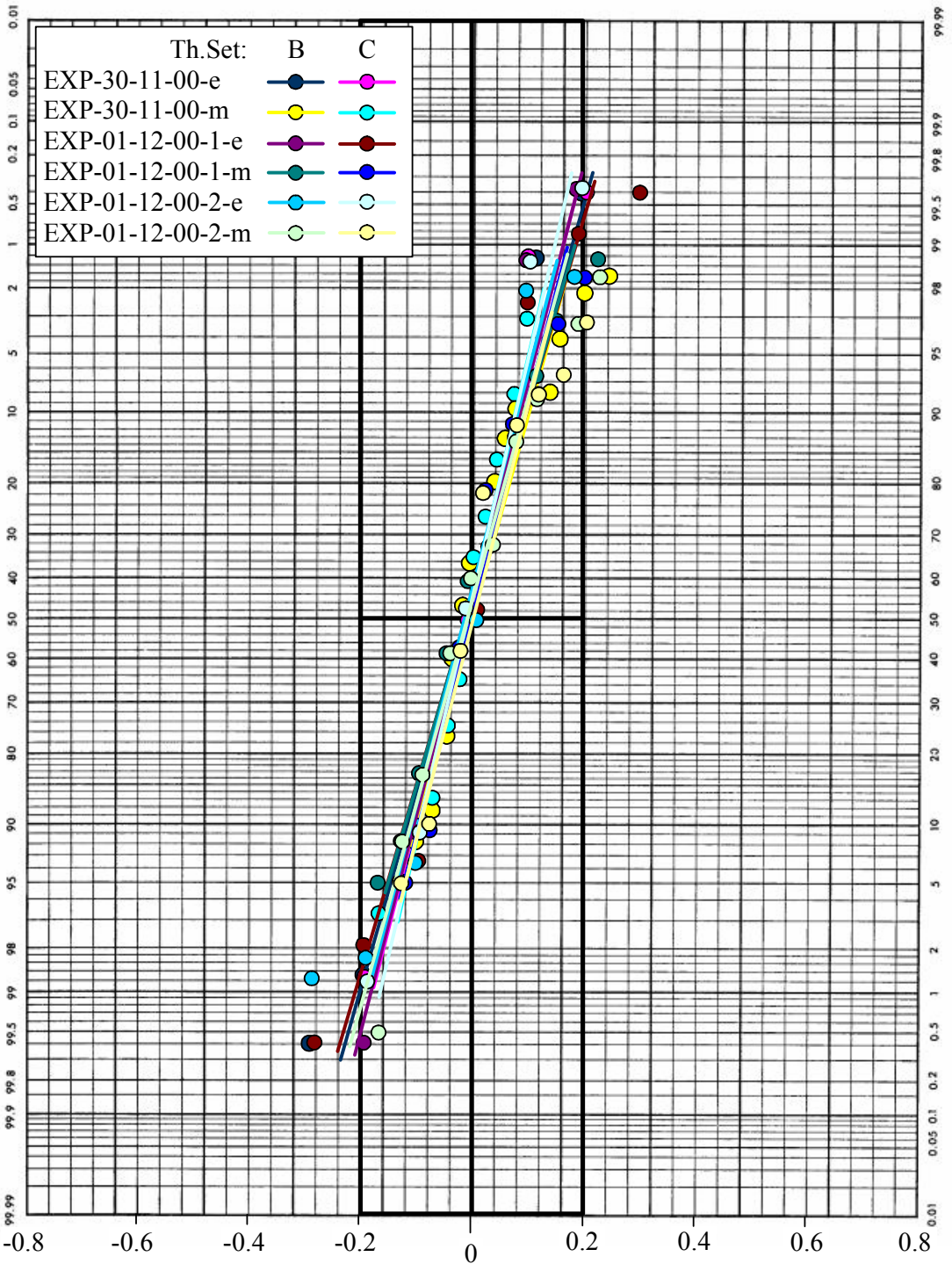

Figure 1.36: Probability check showing that the results follow a normal probability distribution; Th.Set B&C EXP-30-11-00 and EXP-01-12-00.

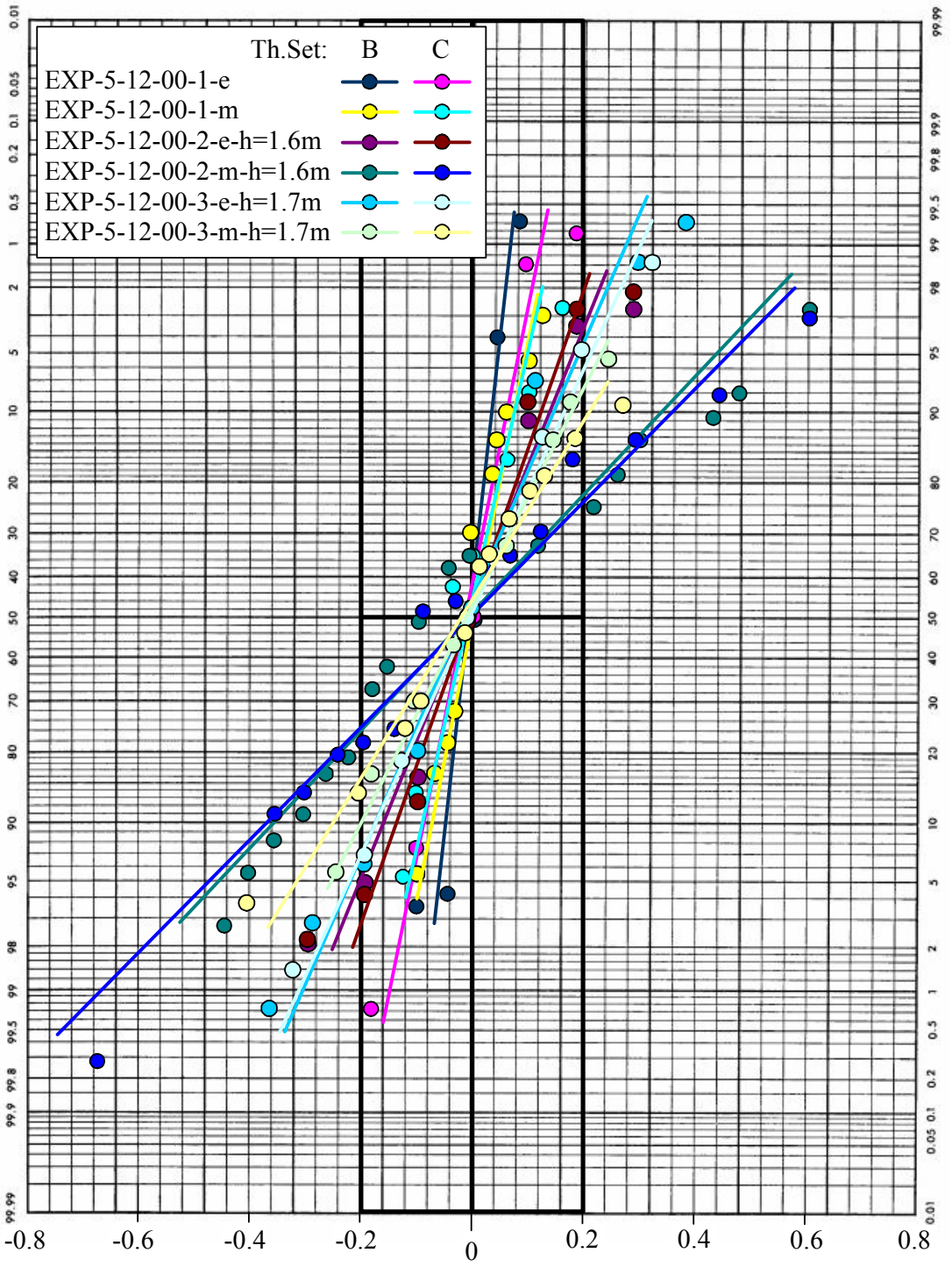

Figure 1.37: Probability check showing that the results follow a normal probability distribution; Th.Set B&C EXP-5-12-00.

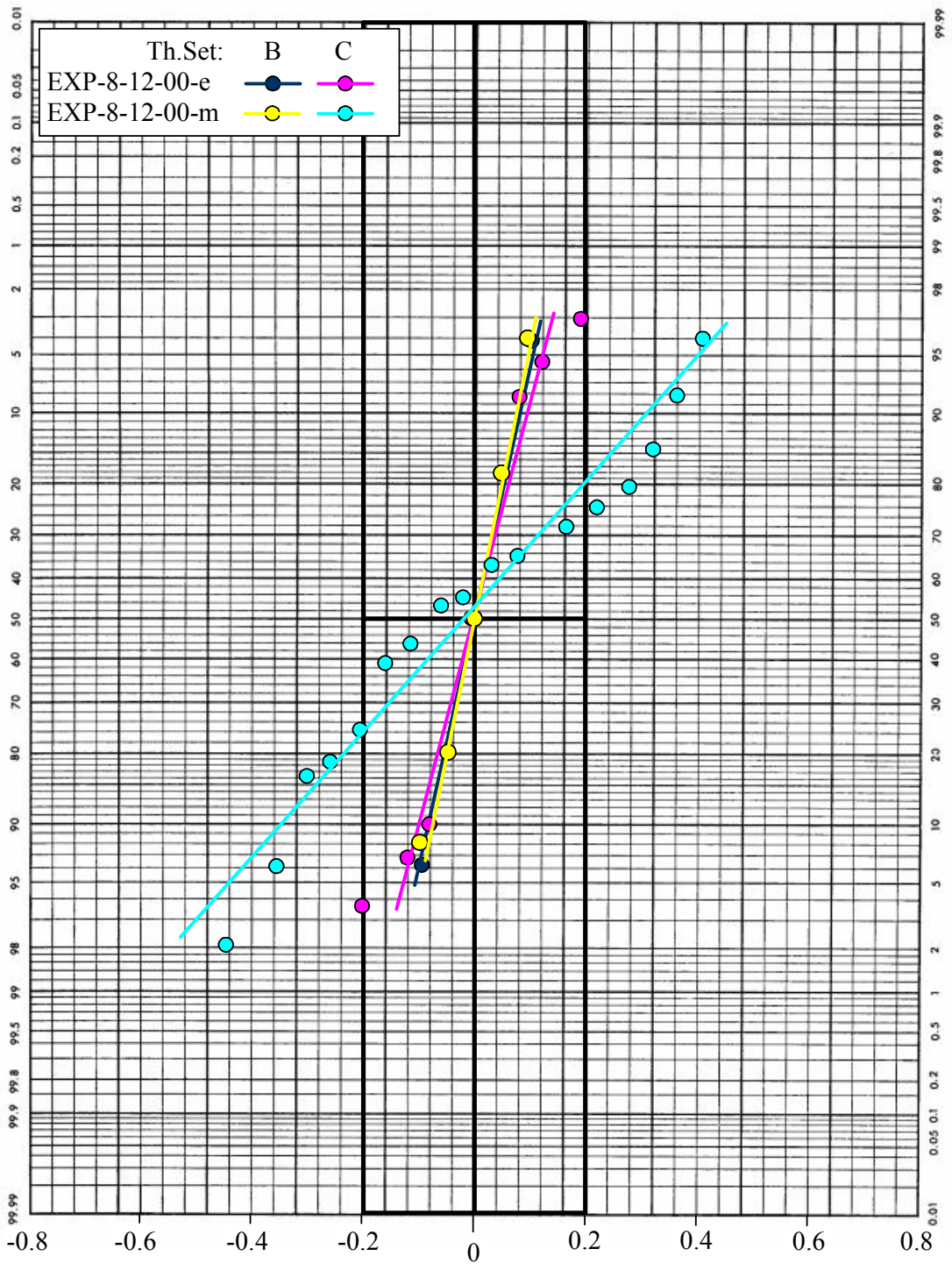
Th.Set: B C
EXP-8-12-00-e
EXP-8-12-00-m
-0.8
-0.6
-0.4
-0.2
0
0.2
0.4
0.6
0.8

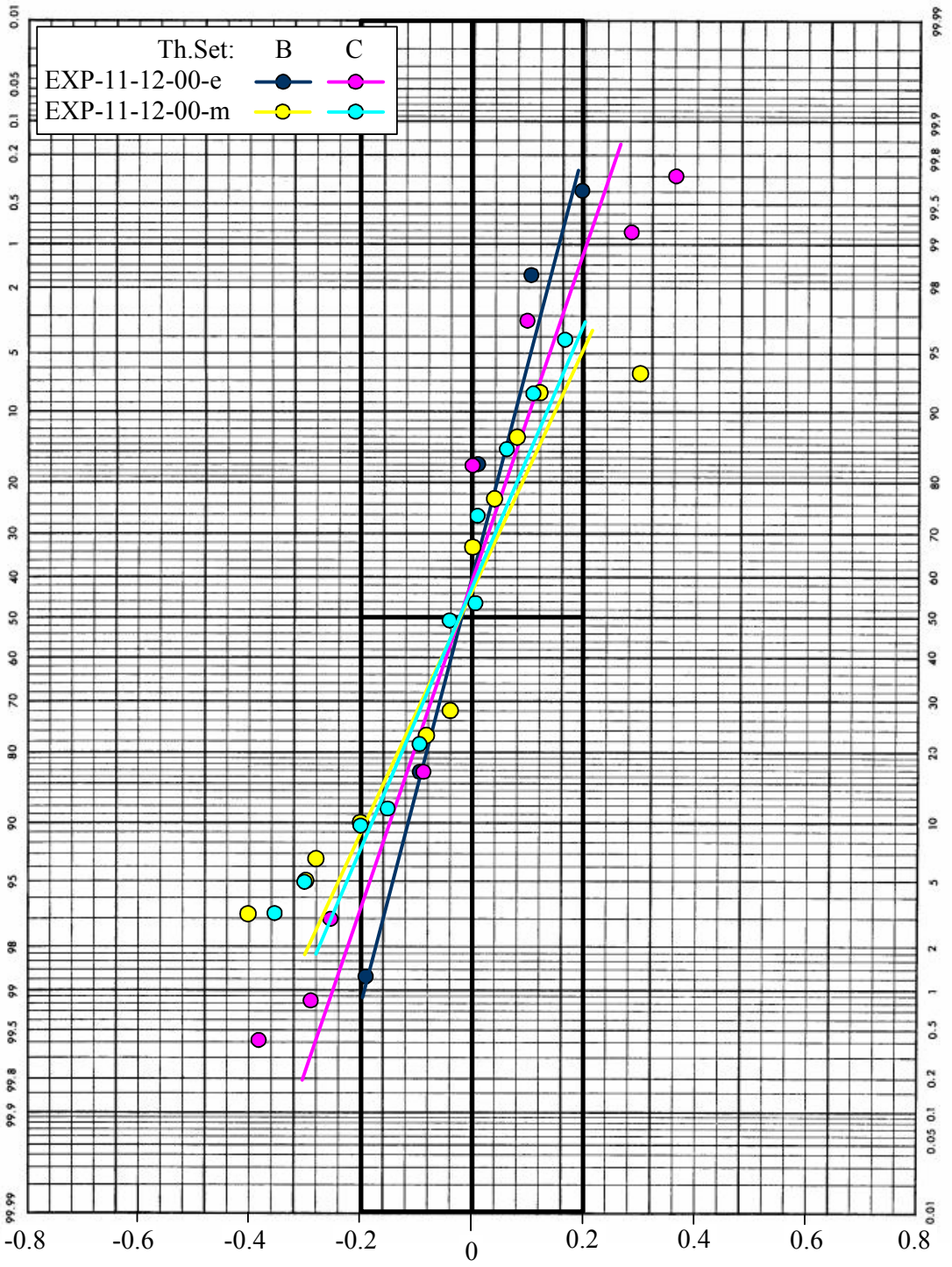

Figure 1.38: Probability check showing that the results follow a normal probability distribution; Th.Set B&C EXP-11-12-00.

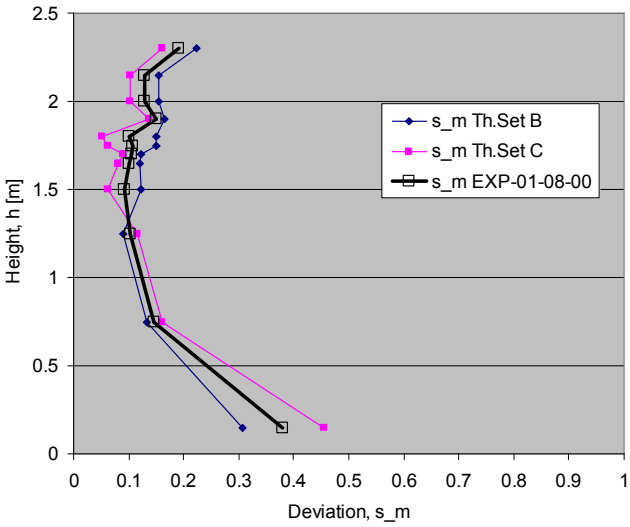

Figure 1.39: case study.